Can low- p_T pion induced Drell-Yan data constrain pion-parton distributions?

Leonard Gamberg

PennState Berks

w/ Patrick Barry, Eric Moffat, Alexei Prokudin
Wally Melnitchouk, Nobuo Sato, Daniel Pitonyak
"JAM 3-D"

CPHI 2022

U.S. DEPARTMENT OF ENERGY | Office of Science

TMD Collaboration

Motivation of my talk

- We explore the impact on JAM 21 pion pdfs extracted from a simultaneous fit of low energy fixed target p_T dependent DY & collinear π-nuclear cross section data

In particular:

- First we carry out a fit of the non-perturbative parameters of the pion TMD from the available data.
- As a second step we open up the fit of both collinear pion pdf parameters along with non-perturbative parameters.
- As a final step, we perform a fit of the p_T integrated and p_T dependent data to carry out a simultaneous fit of the pion collinear pdfs and pion TMDs. This constitutes a first such study.
- We also compare the impact of various scenarios for describing non-perturbative content of the TMD contribution.

The Pion as bound state QCD

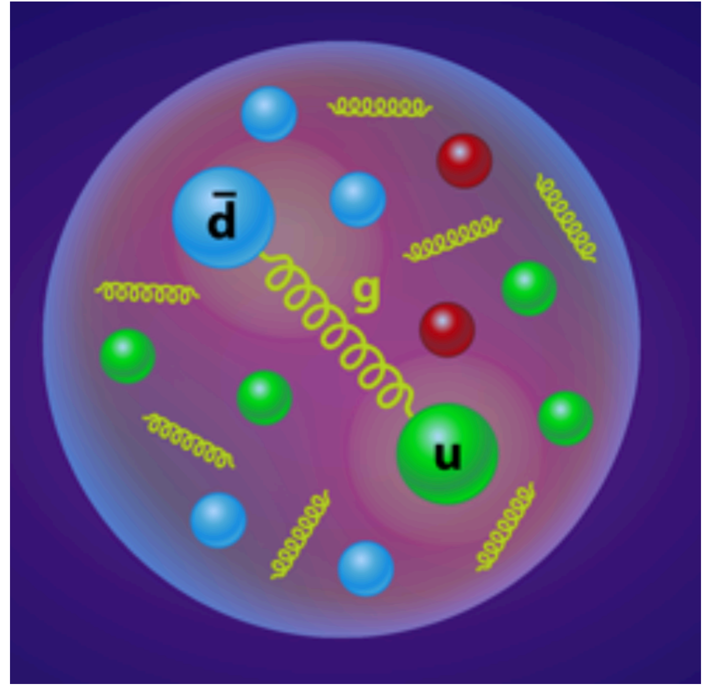

- Pion plays a central/"outsized" role in hadron physics
- @ low energy, as nearly massless $\bar{q}q$ bound state Goldstone boson plays a critical ingredient for understanding dynamical χ symmetry breaking from small current quark masses

Pion pole condition from Bethe-Salpeter

$$m_\pi^2 = \frac{m}{2\,G_\pi\,M\,I(m_\pi^2)}$$

Gell Mann Reiner Oaks Relation

$$f_\pi^2\,m_\pi^2 = \frac{1}{2}\,(m_u + m_d)\,\langle \bar{u}u + \bar{d}d \rangle$$

★ Mass without mass" bulk of pion mass due to QCD quantum fluctuations of $\bar{q}q$ pairs, gluons, & energy associated with quarks moving at close to speed of light

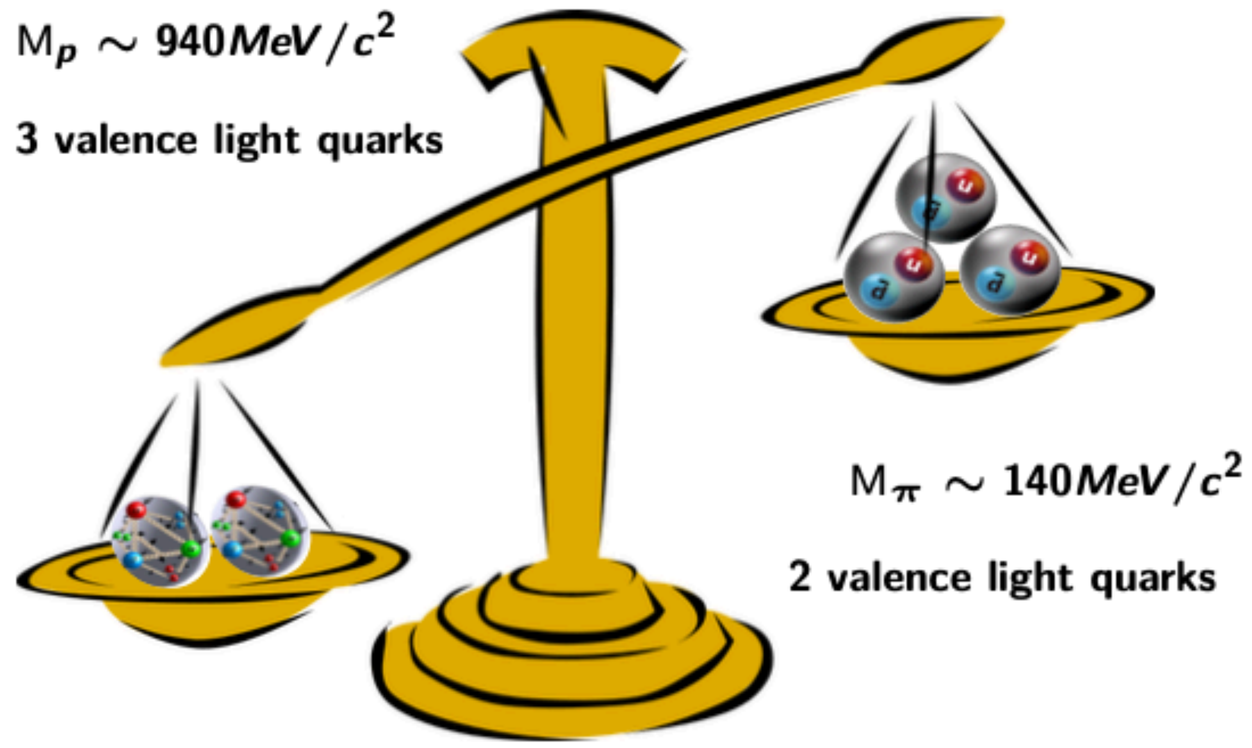

The Pion recent progress

@ high energies pion's partonic structure unfolded/revealed from DY process as predicted from Collinear Factorization ⟶ momentum distributions, $f_{i/\pi}(x, \mu)$

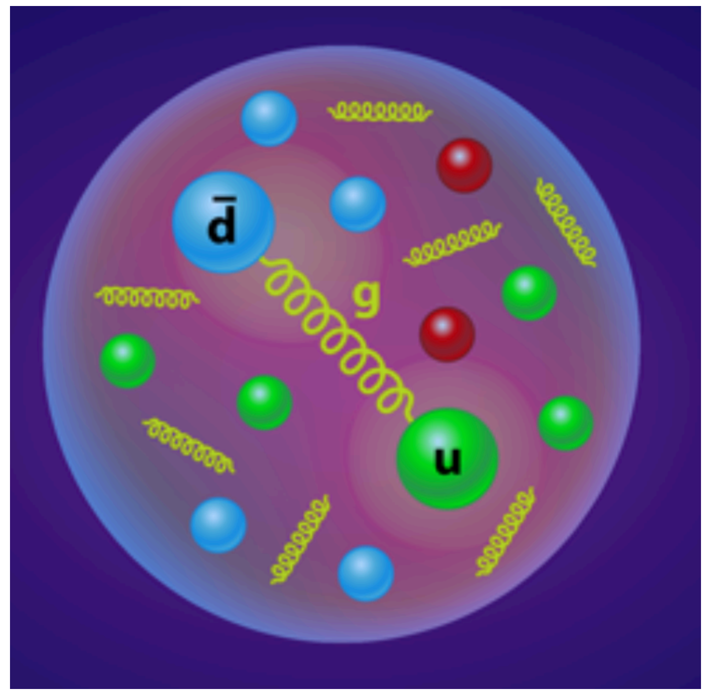

1) $$\frac{d\sigma^{DY}}{dQ^2 dy} = \sum_{a,b} \int dx_a\, dx_b\, H^{DY}_{a,b}(x_a, x_b, y, Q^2, \mu^2)\, f_{a/A}(x_a, \mu^2)\, f_{b/B}(x_b, \mu^2)$$

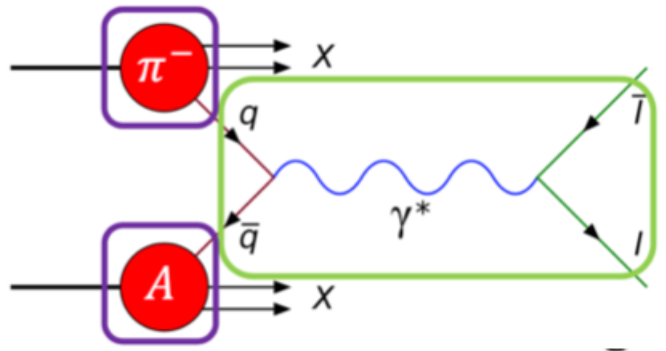

2) $$\frac{d^3\sigma^{LN}}{dx_B\, dQ^2\, dx_L} = \frac{4\pi\alpha^2}{x_B Q^4}\left(1 - y_e + \frac{y_e^2}{2}\right) F_2^{LN}(x_B, Q^2, x_L)$$

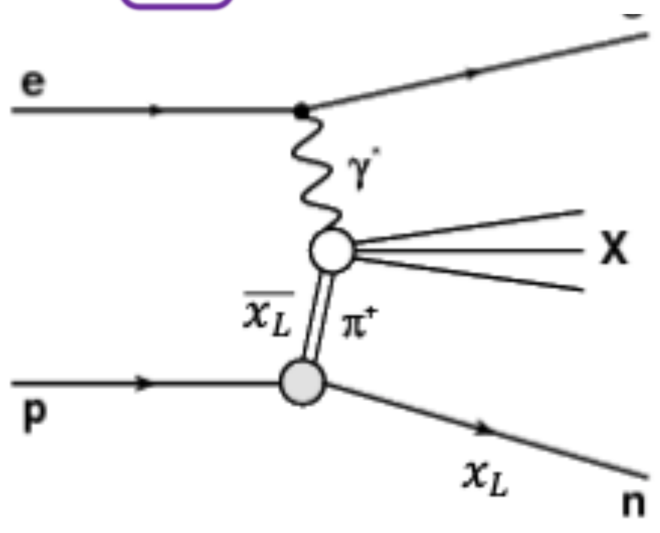

Jefferson Lab Angular Momentum (JAM)

Barry, Sato, Melnitchouk, C.-R. Ji PRL 2018

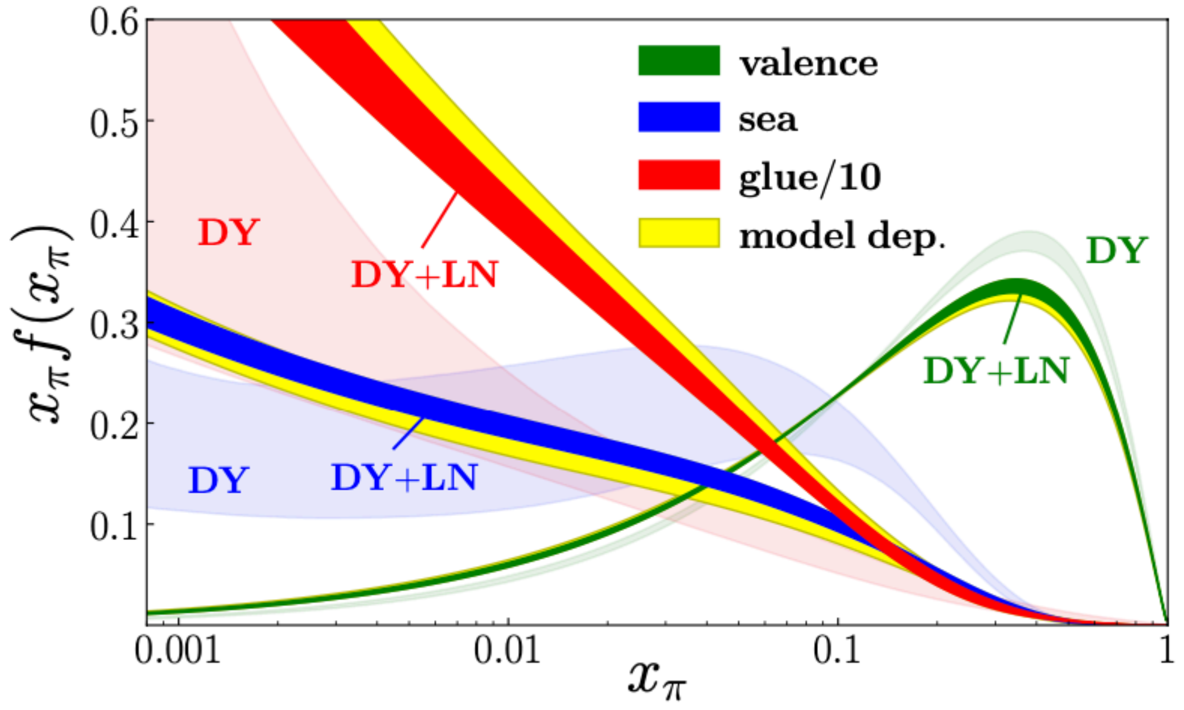

FIG. 2. Pion valence (green), sea quark (blue) and gluon (red, scaled by 1/10) PDFs versus x_π at $Q^2 = 10$ GeV^2, for the full DY + LN (dark bands) and DY only (light bands) fits. The bands represent 1σ uncertainties, as defined in the standard Monte Carlo determination of the uncertainties [42] from the experimental errors. The model dependence of the fit is represented by the outer yellow bands.

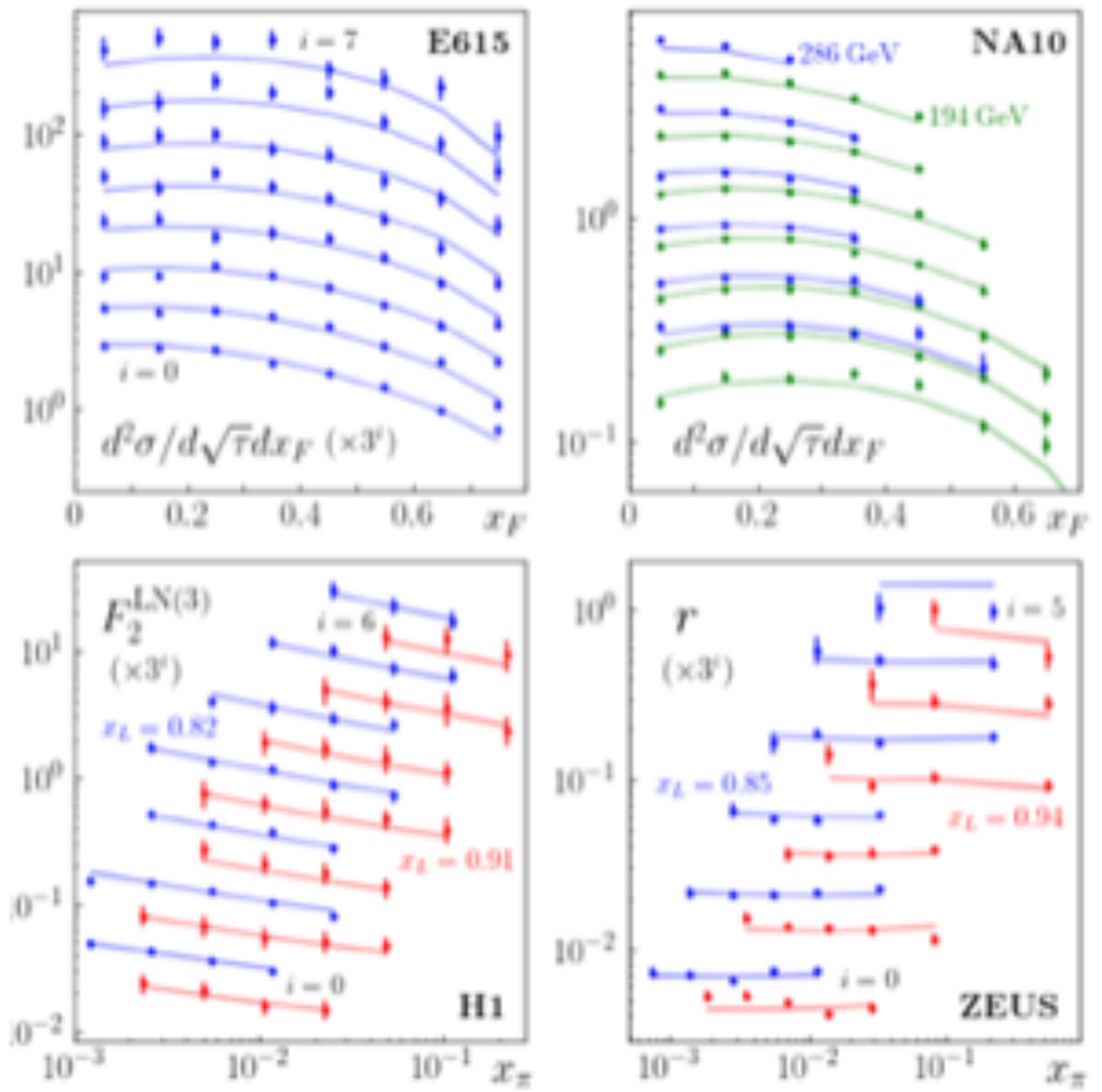

- Top row – Drell-Yan
- Bottom row Leading neutron
- Good agreement with data
- $\chi^2_{\rm npts} = 0.979$

The Pion PDFs progress

Jefferson Lab Angular Momentum (JAM)

Barry, C.R. Ji, Sato, Melnitchouk, PRL 2021

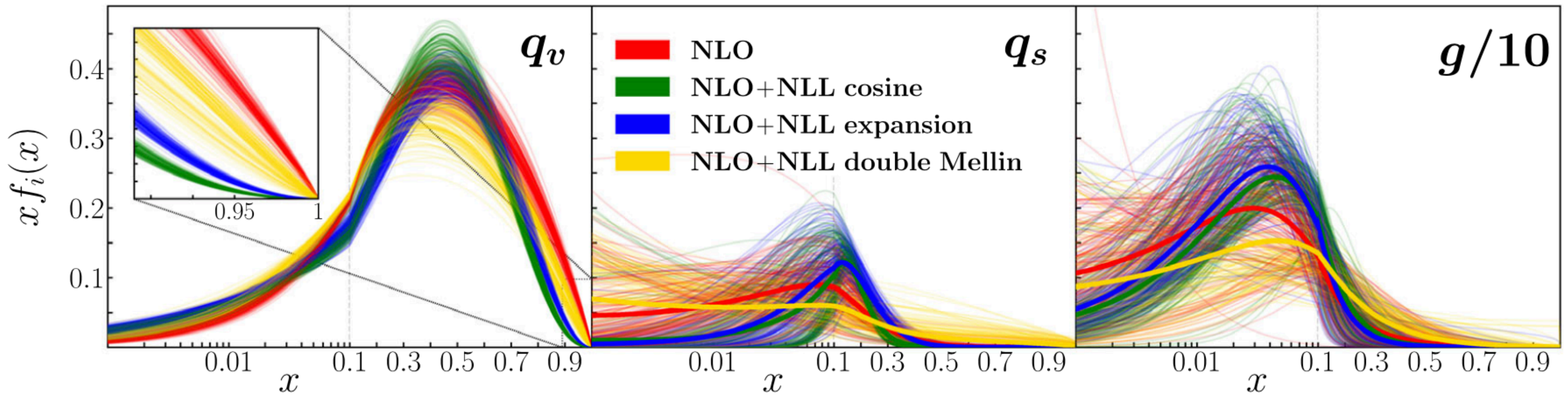

FIG. 2. Distribution of replicas for the pion valence quark (left), sea quark (middle), and gluon ($\times 1/10$) (right) PDFs versus x at the scale μ_0 for the NLO fixed order (red), and NLO + NLL cosine (green), expansion (blue), and double Mellin (gold) analyses. The inset in the left panel magnifies the very large-x region. The central values of the sea quark and gluon posterior samples are indicated by solid lines.

xFitter

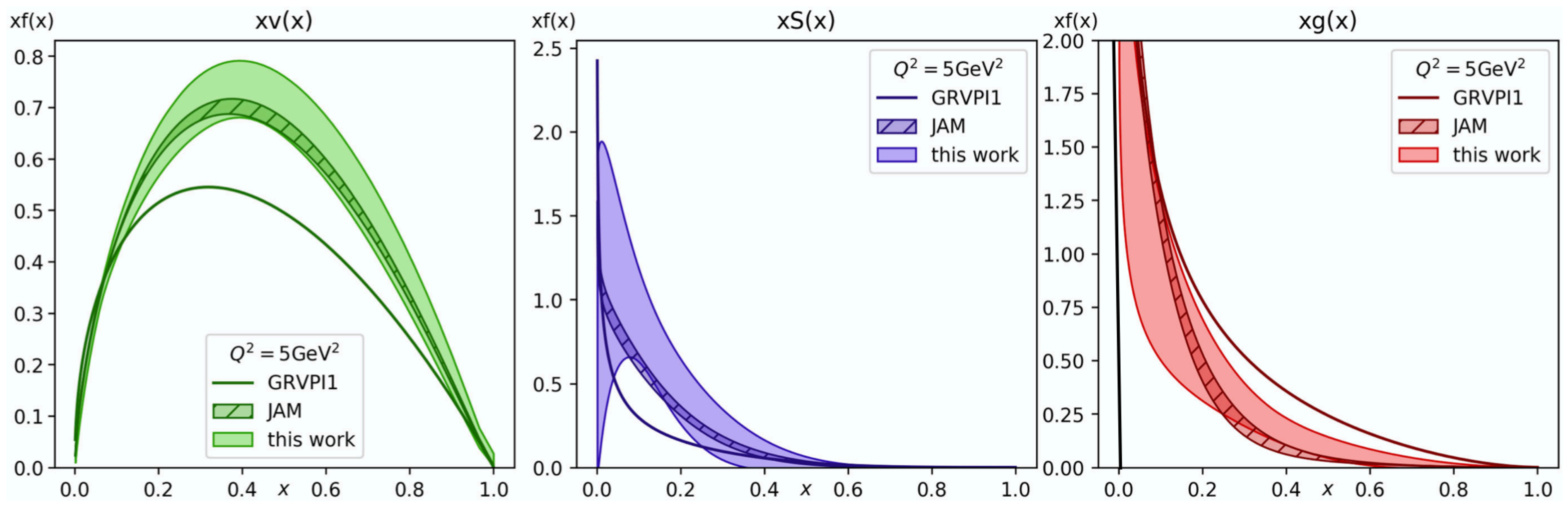

FIG. 3. Comparison between the pion PDFs obtained in this work, a recent determination by the JAM collaboration [31], and the GRVPI1 pion PDF set [27].

Lattice

PRD 2020

RAZA SABBIR SUFIAN *et al.*

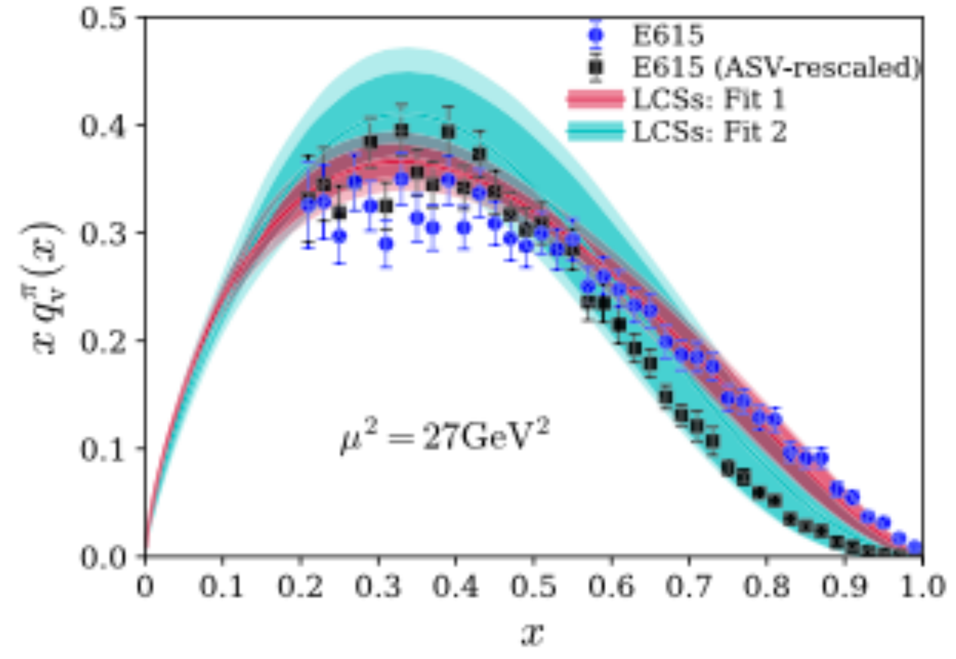

FIG. 8. Comparison of pion $xq_v^\pi(x)$ distribution obtained from this calculation with the $xq_v^\pi(x)$ distributions extracted from the experimental Drell-Yan cross sections. The blue data points are from LO analysis [3] and the "ASV-rescaled" black data points compiled from [71] are the E615 rescaled data according to analysis [11].

Huey-Wen Lin, et al. arXiv 2020

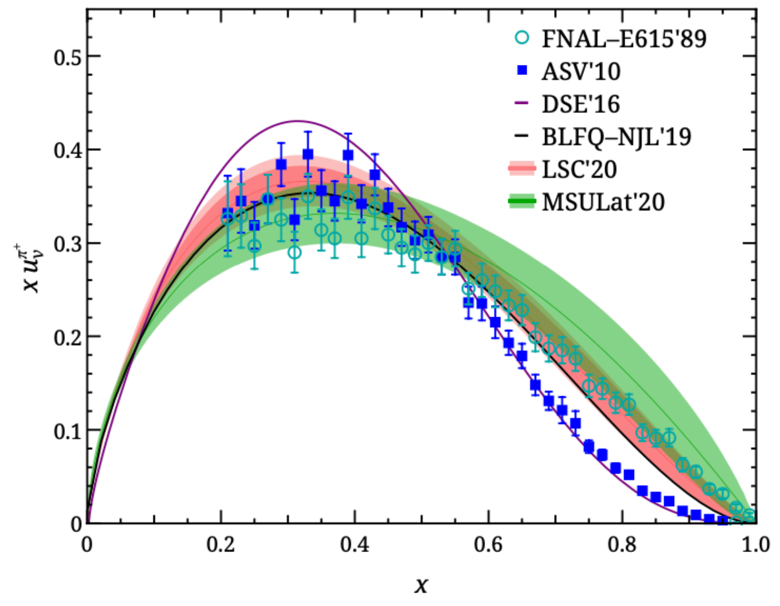

FIG. 6: Summary comparison of xu_v^π as a function of x at scale of 27 GeV^2: our result at physical pion mass (labeled "MSULat'20", shown as a green band), another lattice work using lattice good cross-section method ("LSC'20", shown as a red band) [72] at physical pion mass, along with the original analysis of the FNAL-E615 experiment data [5] ("FNAL-E615'89", cyan circles) and the reanalysis ("ASV'10", blue squares) [7] which agree perfectly with the distribution obtained from Dyson-Schwinger equations ("DSE'16") [71], the obtained from basis light-front quantization with NJL interactions ("BLFQ-NJL'19").

HadStruc

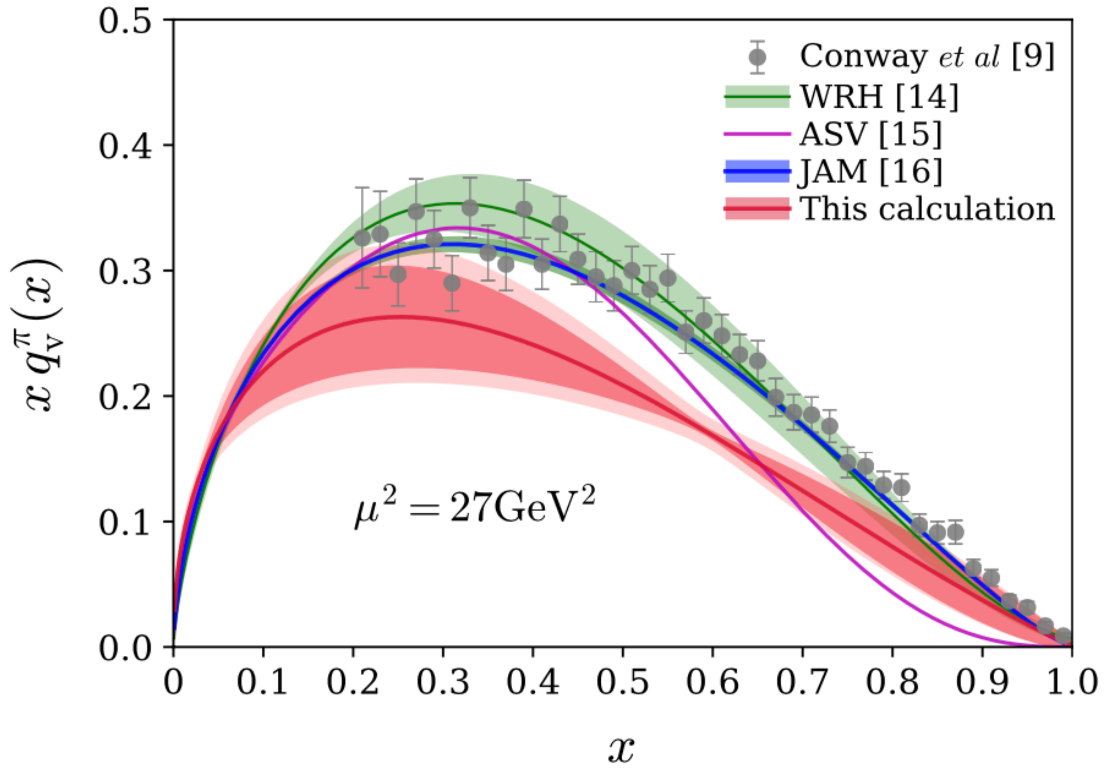

FIG. 13. Comparison of the pion $xq_v^\pi(x)$-distribution with the LO extraction from Drell-Yan data [9] (gray data points with uncertainties), NLO fits [14–16] (green band, maroon curve, and blue band). This lattice QCD calculation of $q_v^\pi(x)$ is evolved from an initial scale $\mu_0^2 = 4$ GeV^2 at NLO. All the results are evolved to an evolution scale of $\mu^2 = 27$ GeV^2. The outer red band shown in the $q_v^\pi(x)$-distribution is obtained from the variation in the choice of α_s during the one-loop perturbative matching as described in Section V and by calculating the variation in the fitting of the matched Ioffe-time data using the PDFs parametrization in Eq. (28).

Extended fit to include "large" p_T Drell Yan data

Cao et al *Phys.Rev.D* 103 (2021), added transverse momentum dependent Drell-Yan data in a global QCD analysis of large transverse momentum $p_T \sim Q$ dominated by hard QCD radiation

3) $$\frac{d\sigma^{\mathrm{DY}}}{dQ^2 dy dp_T} = \sum_{a,b} \int \mathrm{d}x_a \, \mathrm{d}x_b \, H^{\mathrm{FO}}_{a,b}(x_a, x_b, y, p_{\mathrm{T}}, Q^2, \mu^2) \, f_{a/A}(x_a, \mu^2) \, f_{b/B}(x_b, \mu^2)$$

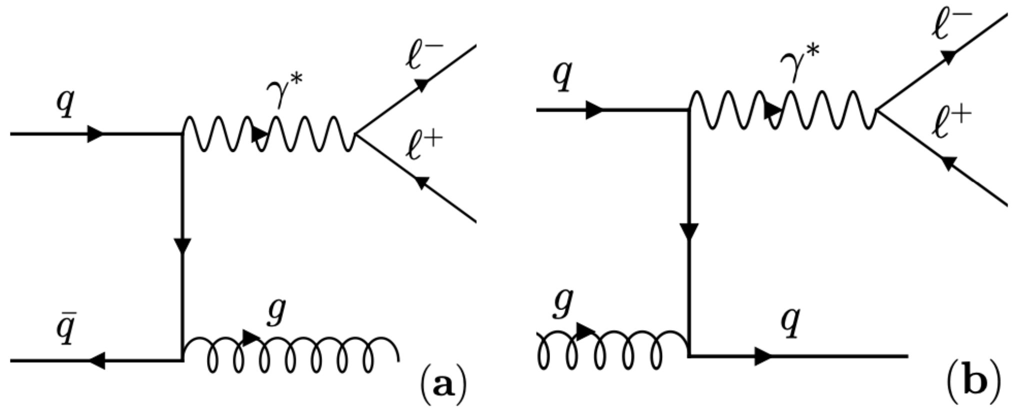

The inclusion of p_{T}-dependent data only slightly reduce uncertainties of the gluon distribution at large x & impacts on other distributions negligible

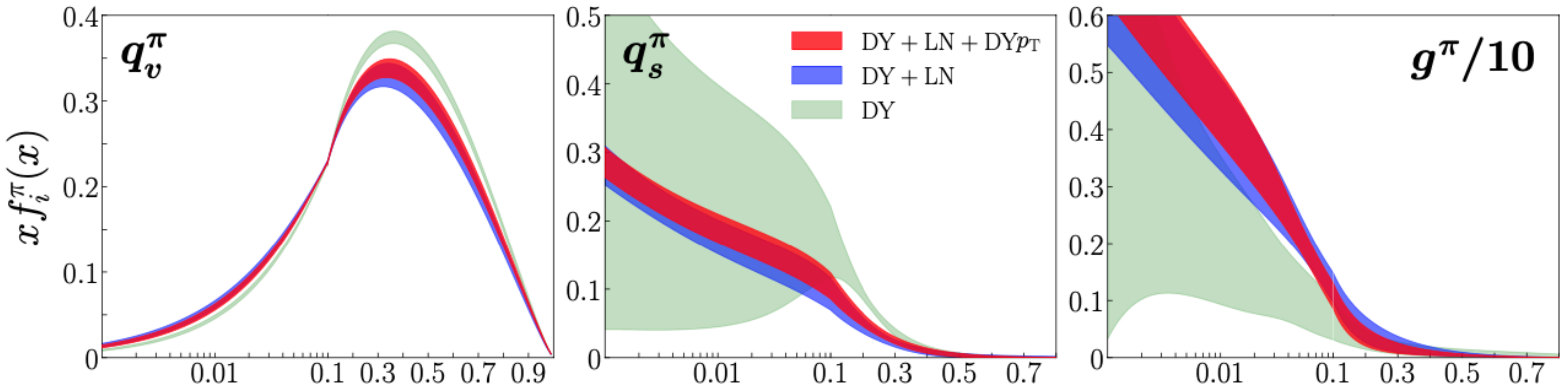

Understanding how these contrasting manifestations of the same $\bar{q}q$ bound state arise dynamically at different energy scales from first principles remains a major challenge in QCD

Extend fit to include "low" p_T Drell Yan data

- We consider impact on collinear pion pdfs from $p_T \sim k_T \ll Q$ "TMD" region (*n.b.* smaller statistical uncertainties on the data)
  - Pion induced DY scattering processes provide possibility to TMDs of the pion and nucleon when the cross section is kept differential in the transverse momentum of the produced lepton pair
  - Factorized according to the framework of Collins-Soper-Sterman (CSS)

"More granular" $p_T \sim k_T \ll Q$ access to the Pion TMDs

To describe the transverse momentum "region" $p_T \sim k_T \ll Q$ is the regime of TMDs of the pion

Requires fitting "region" $p_T \sim k_T \ll Q$ differential pion-induced Drell-Yan cross section

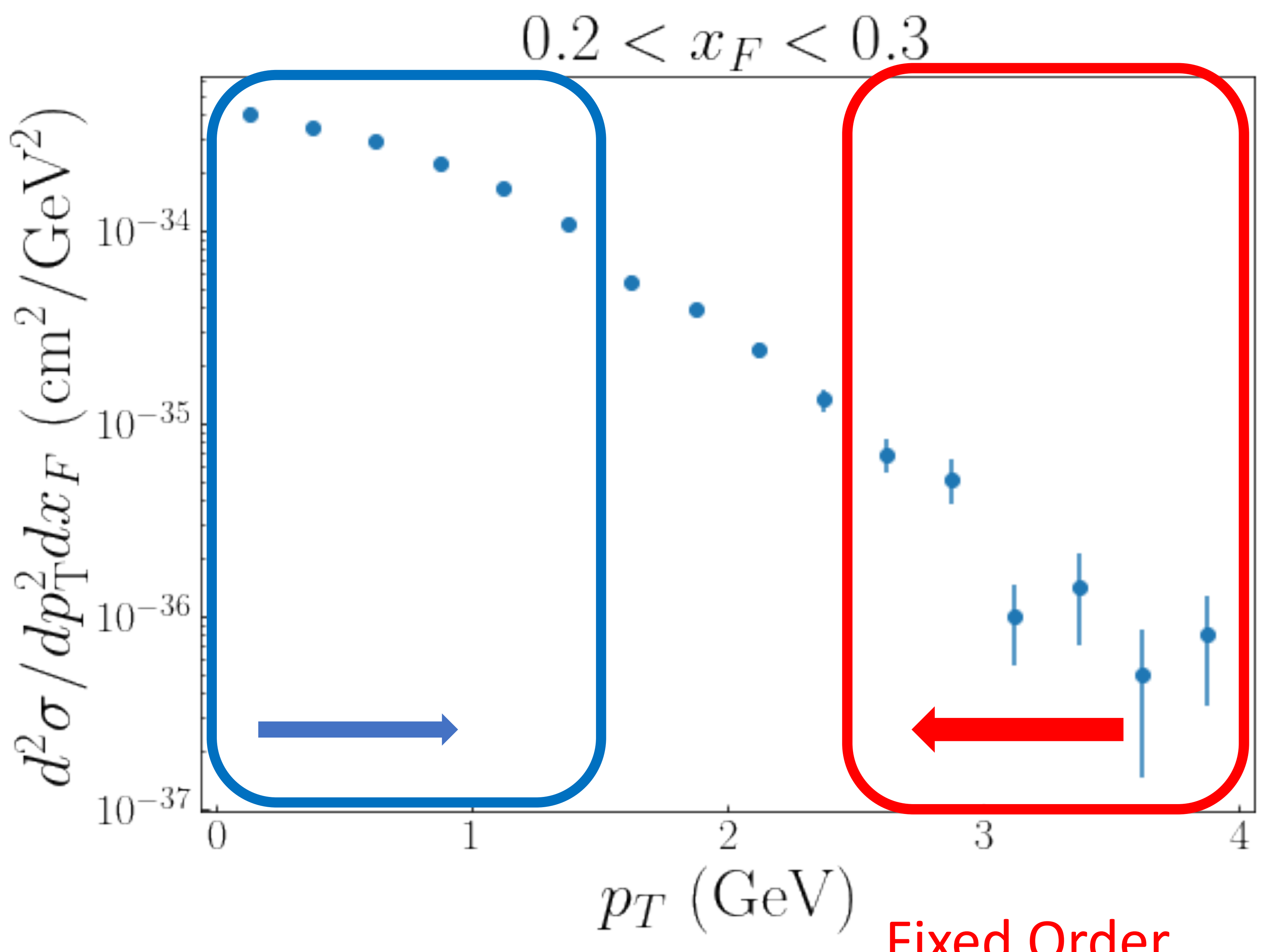

TMD Factorization

Fixed Order Collinear Factorization

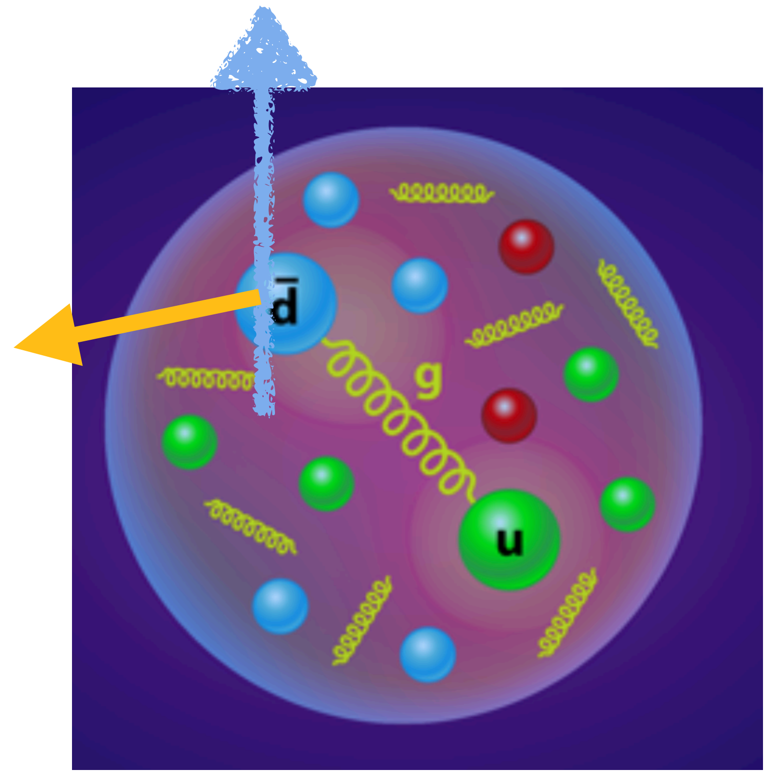

TMD Factorization

$$\frac{d\sigma^W}{dQ^2\, dx_F\, dp_T^2} = \int \frac{d^2\boldsymbol{b}_T}{(2\pi)^2}\, e^{i\boldsymbol{p}_T\cdot\boldsymbol{b}_T}\, \tilde{W}(x_F, b_T, Q)$$

$$\tilde{W}(x_F, b_T, Q) = \sum_j H^{\rm DY}_{j\bar{j}}(Q, \mu, a_s(\mu))\, \tilde{f}_{j/A}(x_A, b_T; \zeta_A, \mu)\, \tilde{f}_{\bar{j}/B}(x_B, b_T; \zeta_B, \mu)$$

First Studies

Vladimirov JHEP 2019

Pion-induced DY processes within TMD factorization

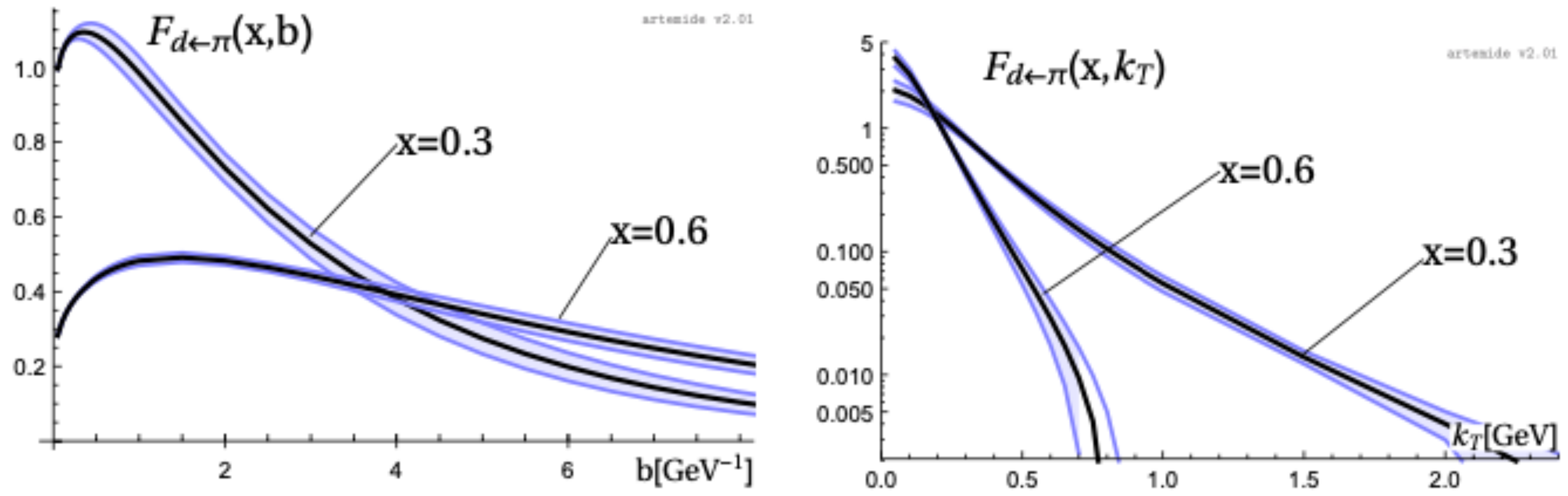

Pion TMDPDF for d-quark in b-space. (Right) Pion TMDPDF for d-quark in kT -space.
The bands are the 1σ uncertainty band related to the data error-bands and calculated by the replica method.

$$\frac{d\sigma^W}{dQ^2\,dx_F\,dp_T^2} = \frac{4\pi^2\alpha^2}{9Q^2 s}\sum_j H_{j\bar{j}}^{\rm DY}(Q,\mu_Q,a_s(\mu_Q))$$

$$\times \int \frac{d^2\boldsymbol{b}_T}{(2\pi)^2}\, e^{i\boldsymbol{p}_T\cdot\boldsymbol{b}_T}\; \tilde{f}_{j/\pi}(x_A,b_T;Q^2,\mu_Q)\; \tilde{f}_{\bar{j}/H}(x_B,b_T;Q^2,\mu_Q)$$

W term zeta prescription No flavor

Scimemi & Vladimirov 2018

Also, see

Ceccopieri, Courtoy,Noguera,. Scopetta, EPJC (2018)

Shi, Bednar, Cloet, Freese PRD 2020

E615 DY Data

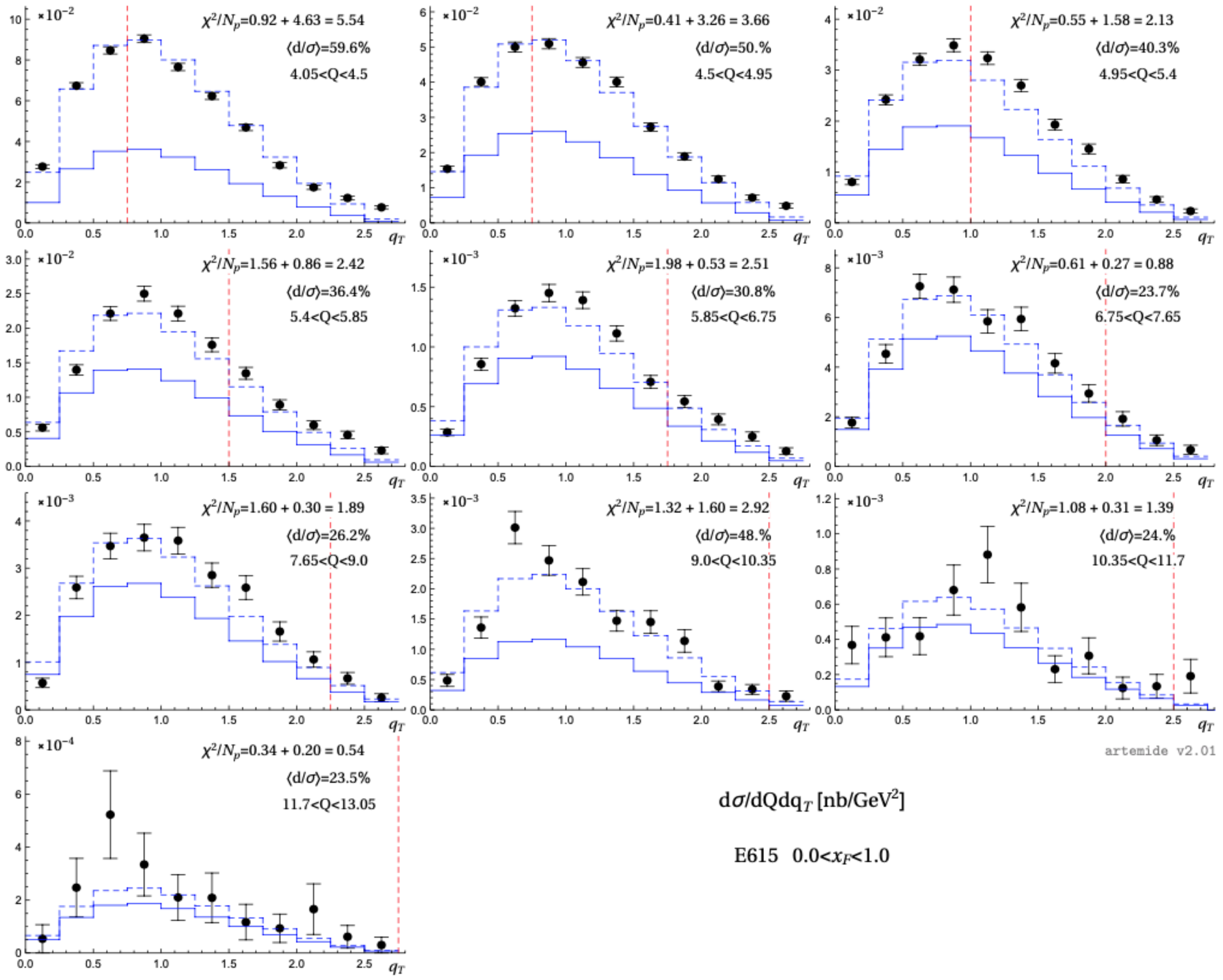

Figure 5. Comparison of the theory prediction (solid line) to E615 differential in Q. The dashed line is the theoretical prediction after the addition of systematic shifts d_i. The values of the χ^2 and d_i are calculated for the each Q-bin with 16% correlated error. The vertical dashed line shows the estimation of the boundary for TMD factorization approach.

The Pion TMDs: factorization, renormalization, and evolution

$q_T \sim k_T \ll Q$

Leading Power TMDPDFs

Quark Spin

TMD Factorization

- ✦Mulders Tangerman NPB1995
- ✦Boer Mulders PRD 1997

	Quark Polarization		
	Un-Polarized (U)	Longitudinally Polarized (L)	Transversely Polarized (T)
[redacted] U	f_1 = Unpolarized		$h_1^\perp$ = − Boer-Mulders

$$f(x, k_T, s_T) = \frac{1}{2}\left[f_1^\pi(x, k_T^2) + \frac{s_T^i \epsilon^{ij} k_T^j}{m_\pi} h_1^{\pi\,\perp}(x, k_T^2)\right]$$

- Factorization carried out Fourier b_T space FT TMDs $\tilde{f}(x, b_T; \zeta, \mu)$
- Real QCD need QFT definitions of TMDs LC & UV divergences reflected in the CS & RG Eqs.
- TMD Evolution depends on rapidity ζ and RGE scales μ

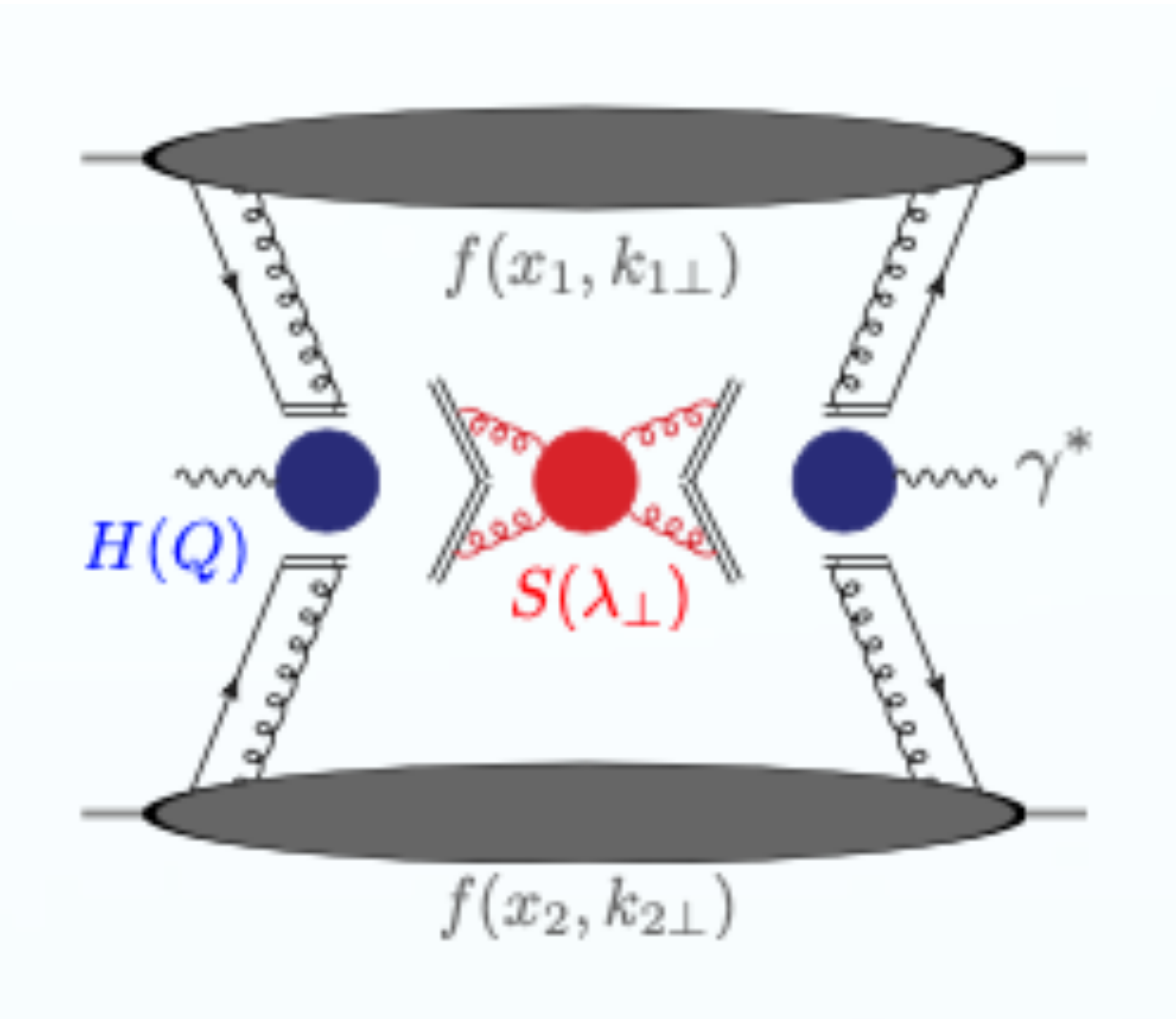

TMD Factorization

- ✦*Collins Soper Sterman NPB 1985*
- ✦*Ji Ma Yuan PRD PLB …2004, 2005*
- ✦*Aybat Rogers PRD 2011*
- ✦*Collins 2011 Cambridge Press*
- ✦*Echevarria, Idilbi, Scimemi JHEP 2012, …*
- ✦*SCET Becher & Neubert, 2011 EJPC*

4W) !!!

$$\frac{d\sigma^W}{dQ^2\, dx_F\, dp_T^2} = \int \frac{d^2\boldsymbol{b}_T}{(2\pi)^2}\, e^{i\boldsymbol{p}_T\cdot\boldsymbol{b}_T}\, \tilde{W}(x_F, b_T, Q)$$

$$\tilde{W}(x_F, b_T, Q) = \sum_j H_{j\bar{j}}^{DY}(Q, \mu, a_s(\mu))\, \tilde{f}_{j/A}(x_A, b_T; \zeta_A, \mu)\, \tilde{f}_{\bar{j}/B}(x_B, b_T; \zeta_B, \mu)$$

Renormalization and TMD Evolution- $\{\zeta, \mu\}$

- Collins Soper Eq. $$\frac{\partial \ln \tilde{f}_{j/H}(x, b_T; \mu, \zeta)}{\partial \ln \sqrt{\zeta}} = \tilde{K}(b_T, \mu)$$

$$\tilde{K}(b_T, \mu) \equiv \frac{1}{2} \frac{\partial}{\partial y_n} \ln \frac{S(b_T, y_n, -\infty)}{S(b_T, y_n, -\infty)}$$

- RGE for C.S. kernel $$\frac{d\tilde{K}(b_T; \mu)}{d \ln \mu} = -\gamma_k(\alpha_s(\mu))$$

- RGE for TMD $$\frac{d \ln \tilde{f}_{j/H}(x, b_T; \mu, \zeta)}{d \ln \mu} = -\gamma_F(\alpha_s(\mu), \zeta/\mu)$$

Solve simultaneously and get evolved renormalized TMD $\rightarrow \zeta = Q^2, \quad \mu = \mu_Q \sim Q$

Evolution Renormalization and TMD $\{\zeta, \mu\}$

$$\tilde{f}_{i/P}(x, \mathbf{b}_T, \mu, \zeta) = \tilde{f}_{i/P}(x, \mathbf{b}_T, \mu_0, \zeta_0) \exp\left\{\int_{\mu_0}^{\mu} \frac{d\mu'}{\mu'} \gamma_q[\alpha_s(\mu'); \zeta_0/\mu'^2]\right\} \exp\left\{\tilde{K}(b_T; \mu) \ln \sqrt{\frac{\zeta}{\zeta_0}}\right\}$$

Integral extends from b =0 to infinity one cannot avoid using parton densities and K in the nonperturbative large-bT region.

CSS evolution *F.T.*-TMD B.C. OPE & b_* prescript.

$$b_*(b_T) \equiv \sqrt{\frac{b_T^2}{1 + b_T^2/b_{\max}^2}}$$

$$\tilde{f}_{i/p}(x, \mathbf{b}_T, \mu, \zeta) = \sum_j \int_x^1 \frac{d\hat{x}}{\hat{x}} \tilde{C}_{i/j}(x/\hat{x}, b_T; \mu_{b_*}, \mu_{b_*}^2, \alpha_s(\mu_{b_*}))\, f_{j/p}(\hat{x}; \mu_{b_*})$$
$$\times \exp\left[\ln \frac{\sqrt{\zeta}}{\mu_{b_*}} \tilde{K}(b_*, \mu_{b_*}) + \int_{\mu_{b_*}}^{\mu} \frac{d\mu'}{\mu'} \left(\gamma_q[\alpha_s(\mu'); 1] - \ln \frac{\sqrt{\zeta}}{\mu'} \gamma_K[\alpha_s(\mu_{b_*})]\right)\right]$$
$$\times \exp\left[-g_{i/p}(x, b_T) - \ln\left(\sqrt{\frac{\zeta}{\zeta_0'}}\right) g_K(b_T; b_{\max})\right].$$

CSS evolution *F.T.*-TMD B.C. OPE & b_* prescript.

Solution w/ evolution

$$\tilde{f}_1(x, b_T, Q^2, \mu_Q) \sim \left[\tilde{C}^{f_1}\left(x/\hat{x}, \boldsymbol{b}_*; \mu_{b_*}^2, \mu_{b_*}, \alpha(\mu_{b_*})\right) \otimes f_1(\hat{x}, \mu_{b_*})\right]$$

$$\times \exp\left[-S_{pert}(\mu_{b_*}(b_T); \mu_{b_*}, Q^2) - S_{NP}(b_T, Q)\right]$$

perturbative Sudakov factor

$$\underbrace{-\ln(Q/\mu_{b_*})\tilde{K}(b_*, \mu_{b_*}) - \int_{\mu_{b_*}}^{\mu_Q} \frac{d\mu'}{\mu'}\left[\gamma(\alpha_s(\mu'); 1) - \gamma_K(\alpha_s(\mu'))\ln(Q/\mu')\right]}_{\text{same for unpol. and pol.}}$$

non-perturbative Sudakov factor

$$g_{f_1}(x, b_T) + g_K(b_T)\ln(Q/Q_0)$$

different for each TMD

universal

$$b_*(b_T) \equiv \sqrt{\frac{b_T^2}{1 + b_T^2/b_{\max}^2}} \qquad \mu_{b_*} = C_1/b_*(b_T)$$

TMD factorization

W – term

- In small-p_{T} region, Use the CSS formalism for TMD evolution

$$\frac{d\sigma}{dQ^2\,dy\,dq_{\mathrm{T}}^2} = \frac{4\pi^2\alpha^2}{9Q^2 s} \sum_{j,j_A,j_B} H^{\mathrm{DY}}_{j\bar{j}}(Q,\mu_Q,a_s(\mu_Q)) \int \frac{d^2\boldsymbol{b}_{\mathrm{T}}}{(2\pi)^2} e^{i\boldsymbol{q}_{\mathrm{T}}\cdot\boldsymbol{b}_{\mathrm{T}}}$$
$$\times e^{-\boxed{g_{j/A}(x_A,b_{\mathrm{T}};b_{\max})}} \int_{x_A}^1 \frac{d\xi_A}{\xi_A} f_{j_A/A}(\xi_A;\mu_{b_*}) \tilde{C}^{\mathrm{PDF}}_{j/j_A}\left(\frac{x_A}{\xi_A}, b_*;\mu^2_{b_*},\mu_{b_*},a_s(\mu_{b_*})\right)$$
$$\times e^{-\boxed{g_{\bar{j}/B}(x_B,b_{\mathrm{T}};b_{\max})}} \int_{x_B}^1 \frac{d\xi_B}{\xi_B} f_{j_B/B}(\xi_B;\mu_{b_*}) \tilde{C}^{\mathrm{PDF}}_{\bar{j}/j_B}\left(\frac{x_B}{\xi_B}, b_*;\mu^2_{b_*},\mu_{b_*},a_s(\mu_{b_*})\right)$$
$$\times \exp\left\{-\boxed{g_K(b_{\mathrm{T}};b_{\max})}\ln\frac{Q^2}{Q_0^2} + \tilde{K}(b_*;\mu_{b_*})\ln\frac{Q^2}{\mu^2_{b_*}} + \int_{\mu_{b_*}}^{\mu_Q}\frac{d\mu'}{\mu'}\left[2\gamma_j(a_s(\mu')) - \ln\frac{Q^2}{(\mu')^2}\gamma_K(a_s(\mu'))\right]\right\}$$

Non-perturbative TMDs to extract

Aybat Rogers 2011 & Collins 2011

- Perturbative content calculated from first principles of QFT
- Non-perturbative Collinear pdfs &
- TMD to be fit to data

Considering
Non-perturbative Universal content schemes

$$e^{-g_k(b_T;b_{max})\log\left(\frac{Q}{Q_0}\right)}$$

- Perturbative content calculated from first principles of QFT
- Non-perturbative content (as for collinear case) to be fit

$$g_K(b_T;b_{max}) = \frac{g_2 b_{NP}^2}{2}\ln\left(1+\frac{b_T^2}{b_{NP}^2}\right) = g_2 b_{NP}^2 \ln\frac{b_T}{b_*}$$

$$\lim_{b_T\to 0} g_K(b_T;b_{max}) \approx \frac{g_2}{2}b_T^2$$

Aidala, Field, Gamberg, Rogers PRD 2014 “Large b_T“
Sun, Yuan 2015, used in many pheno analyses

$$g_k(b_T;b_{max}) = \frac{g_2}{2}b_T b_*$$

Vladimirov JHEP 2019 “Large b_T“

$$g_k(b_T;b_{max}) = g_0\left(1-\exp\left[-\frac{C_F\alpha_s(\mu_{b*})b_T^2}{\pi g_0(b_{max})b_{max}^2}\right]\right)$$

Collins Rogers PRD 2015 “Large b_T“

Considering Non-perturbative “intrinsic” content schemes

$$\boxed{\tilde{f}^{j}_{NP}(b_T, x, Q) = e^{-g_j(x, b_T; b_{max})}}$$

- Perturbative content calculated from first principles of QFT
- Non-perturbative content (as for collinear case) to be fit

- $$\tilde{f}^{j}_{NP}(b_T, x, Q) = \left(\frac{b_*}{b_T}\right)^{2-\nu} \frac{K_{1-\nu}\left(M b_T\, x^{g_1}(1-x)^{g_4}\right) \times (1 + C_A b_T + C_B/b_T)}{K_{1-\nu}\left(M b_*\, x^{g_1}(1-x)^{g_4}\right) \times (1 + C_A b_* + C_B/b_*)}$$
  Bessel parametrization Aidala Gamberg Rogers 2014
  large exponential behavior $b_T \sim$ advocated Collins Rogers 2014

- $$e^{-g_j(x, b_T; b_{max})} \qquad g_j(x, b_T) = \frac{(\lambda_1(1-x) + \lambda_2 x + \lambda_3 x(1-x))\, b_T^2}{\sqrt{1 + \lambda_4 x^{\lambda_5} b_T^2}}$$
  Vladimirov JHEP 2019 has large exponential behavior in b_T

- $$e^{-g_j(x, b_T; b_{max})} \qquad g_j(x, b_T) = b_T^2 \left(\frac{g_1}{2} + g_1 g_3 \log\left(\frac{10 x x_0}{(x + x_0)}\right)\right)$$
  Aybat Rogers 2011
  generalization of Landry et al.
  2001...

- $$F^{NP}_{QZ}(b, Q, x_A, x_B; b_{max}) = \exp\left\{ -\ln\left(\frac{Q^2 b^2_{max}}{c^2}\right)\{g_1[(b^2)^{\alpha} - (b^2_{max})^{\alpha}] + g_2(b^2 - b^2_{max})\} - \bar{g}_2(b^2 - b^2_{max}) \right\}$$
  Qiu & Zhang PRL 2001 effectively g_k and g_j contained

- $$f_{\rm NP}(x, b_T, \zeta) = \left[\frac{1-\lambda}{1 + g_1(x)\frac{b_T^2}{4}} + \lambda \exp\left(-g_{1B}(x)\frac{b_T^2}{4}\right)\right] \times \exp\left[-(g_2 + g_{2B} b_T^2) \ln\left(\frac{\zeta}{Q_0^2}\right)\frac{b_T^2}{4}\right],$$
  Bacchetta et al 2019 JHEP …

TMD MC analysis – low energy pA & then π A Drell-Yan data

Using Scheme "2" show some prelim results

$$\frac{d\sigma}{dp_T^2 dy dQ^2} = \sigma_0 \sum_{i,j} H_{i,j} \int_0^\infty db_T b_T J_0(p_T b_T) \times \mathrm{OPE}_{i/A} \times \mathrm{OPE}_{j/B}$$
$$\times e^{S_{\rm pert}} \times f_{i/A}^{\rm NP}(x_A, b_T) f_{j/B}^{\rm NP}(x_B, b_T) \times \left(\frac{Q^2}{Q_0^2}\right)^{-g_K}$$

$$g_{j/h}(x, b_T) = \frac{({\lambda_1}^j(1-x) + {\lambda_2}^j x + {\lambda_3}^j x(1-x))b_T^2}{\sqrt{1 + {\lambda_4}^j x^{{\lambda_5}^j} b_T^2}}$$

$$g_K(b_T; b_{\rm max}) = \frac{g_2}{2} b_T b_*$$

With flavor dependence j ${\lambda_n}^j$

P: u,d, s=sea, g=0 15

π^- : valence (ubar=d), u= sea 10

g_2

Aspects of the fit

- Fit to all low energy pA data, where 4< Q< 9 GeV
- Fit to all low energy πA data, where 4< Q< 9 GeV

- Random starting points in parameter space for TMD parameters
- Also, cut on $p_{T\,max} = 0.25\ Q$

Fixed Target Data only!

Pion data

- **E615 DY Data(E537 also)**

Proton data

- **E288 (3 different energies)**
- **E605**

Multi-step procedure

Step #	Datasets	Open distributions	Frozen distributions
1	pA DY	g_j^p g_K	proton PDFs
2	πA DY low energy low p_T	g_j^π	pion PDFs, g_j^p, g_K, proton PDFs
3	pA, πA DY low energy low p_T	g_j^p g_j^π g_K	pion PDFs, proton PDFs
4	πA DY (p_T dependent and p_T integrated)	q_v^π	q_s^π g_{gluon}^π g_j^p g_j^π g_K proton PDFs
5	πA DY (p_T dependent and p_T integrated) and LN	pion PDFs (q_v^π q_s^π g_{gluon}^π	g_j^p g_j^π g_K proton PDFs
6	πA DY (p_T dependent and p_T integrated) and LN	pion PDFs, g_j^π	g_j^p g_K proton PDFs
7	πA DY (p_T dependent and p_T integrated) and LN, pA DY	pion PDFs, g_j^π, + g_K	g_j^p, proton PDFs
8	πA DY (p_T dependent and p_T integrated) and LN, pA DY	pion PDFs, g_j^π g_K + g_j^p	proton PDFs

Results from pA data fits

- **E288 (3 different energies)**
- **E605**

Process	Experiment	Observable	N_{dat}	$\overline{\chi}^2$
***pA* DY**	E288 (200 GeV)	$Ed^3\sigma/dp^3$	38	1.04
	E288 (300 GeV)	$Ed^3\sigma/dp^3$	38	1.49
	E288 (400 GeV)	$Ed^3\sigma/dp^3$	34	1.38
	E605	$Ed^3\sigma/dp^3$	19	1.56

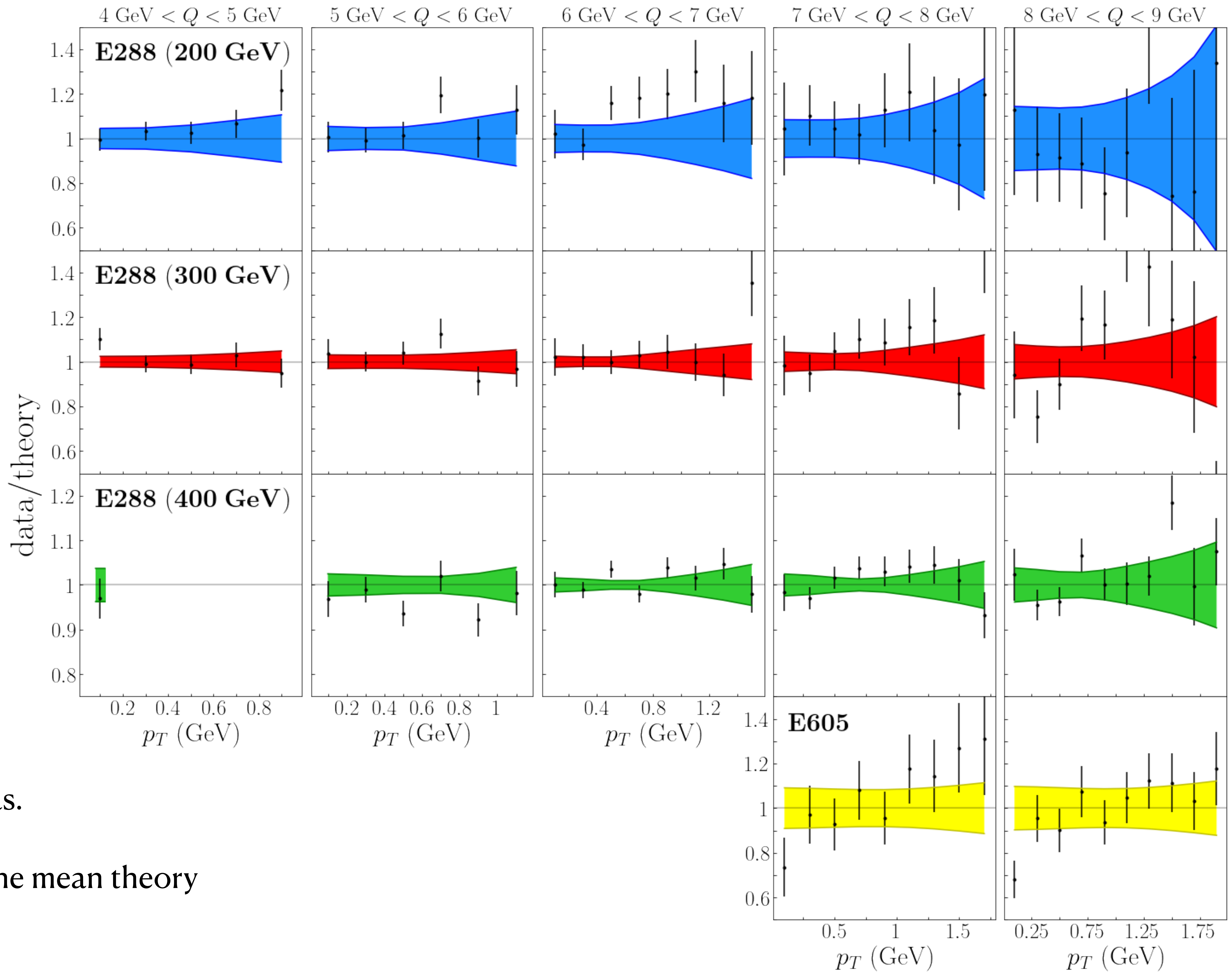

Average theory means the mean value of the observable across all replicas.
Error bar is the uncertainty of the data divided by the mean theory
The band is the 1sigma theory uncertainty across all replicas relative to the mean theory

Results from πA data fits

πA DY	E615	$d^2\sigma/dQdp_\mathrm{T}$	39	4.21
	E615	$d^2\sigma/dx_Fdp_\mathrm{T}$	48	1.46
	E537	$d^2\sigma/dQdp_\mathrm{T}^2$	37	0.80
	E537	$d^2\sigma/dx_Fdp_\mathrm{T}^2$	45	1.00

x_F dependent observable (integrated over Q)

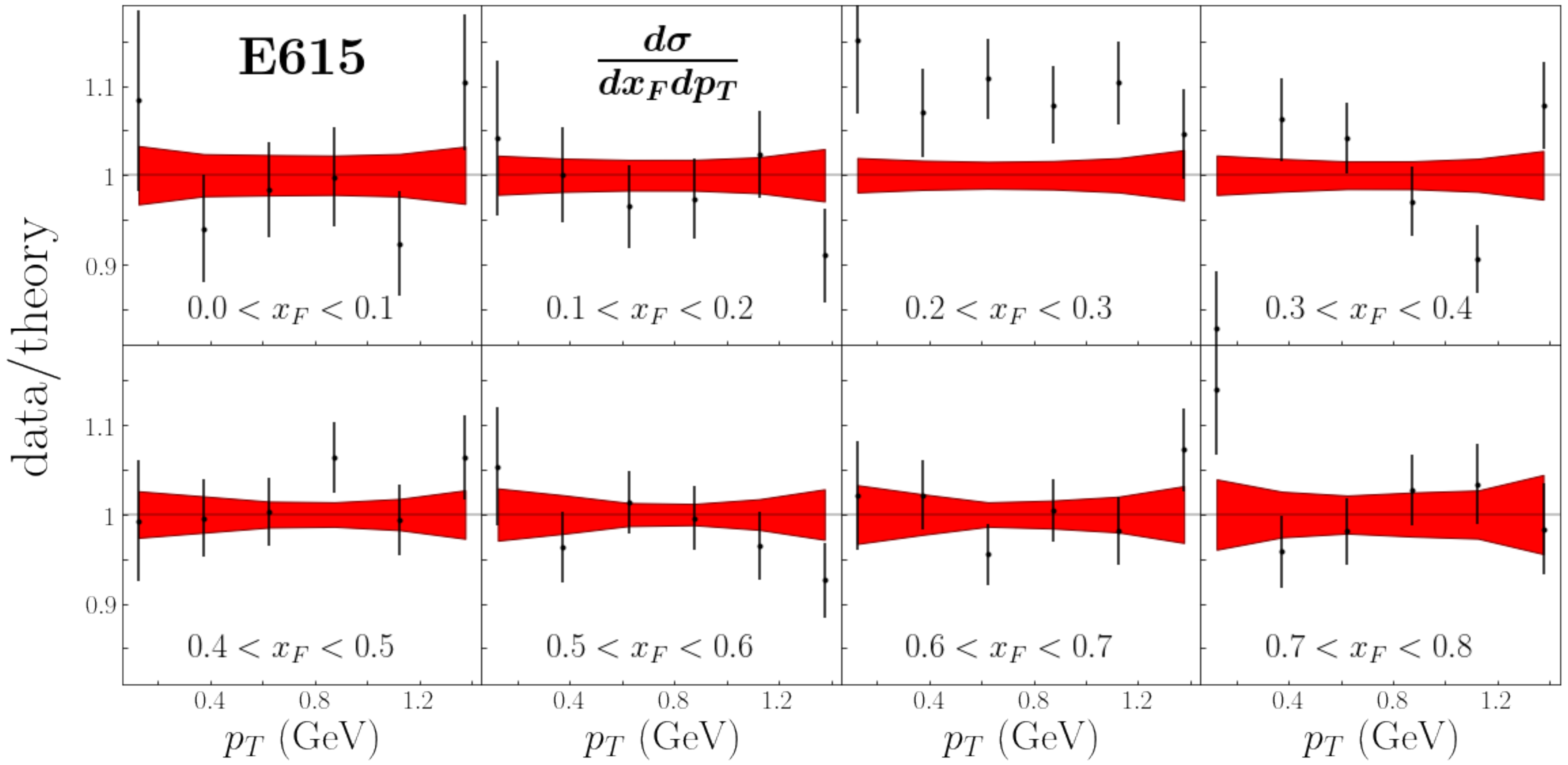

Q^2 dependent observable (integrated over y)

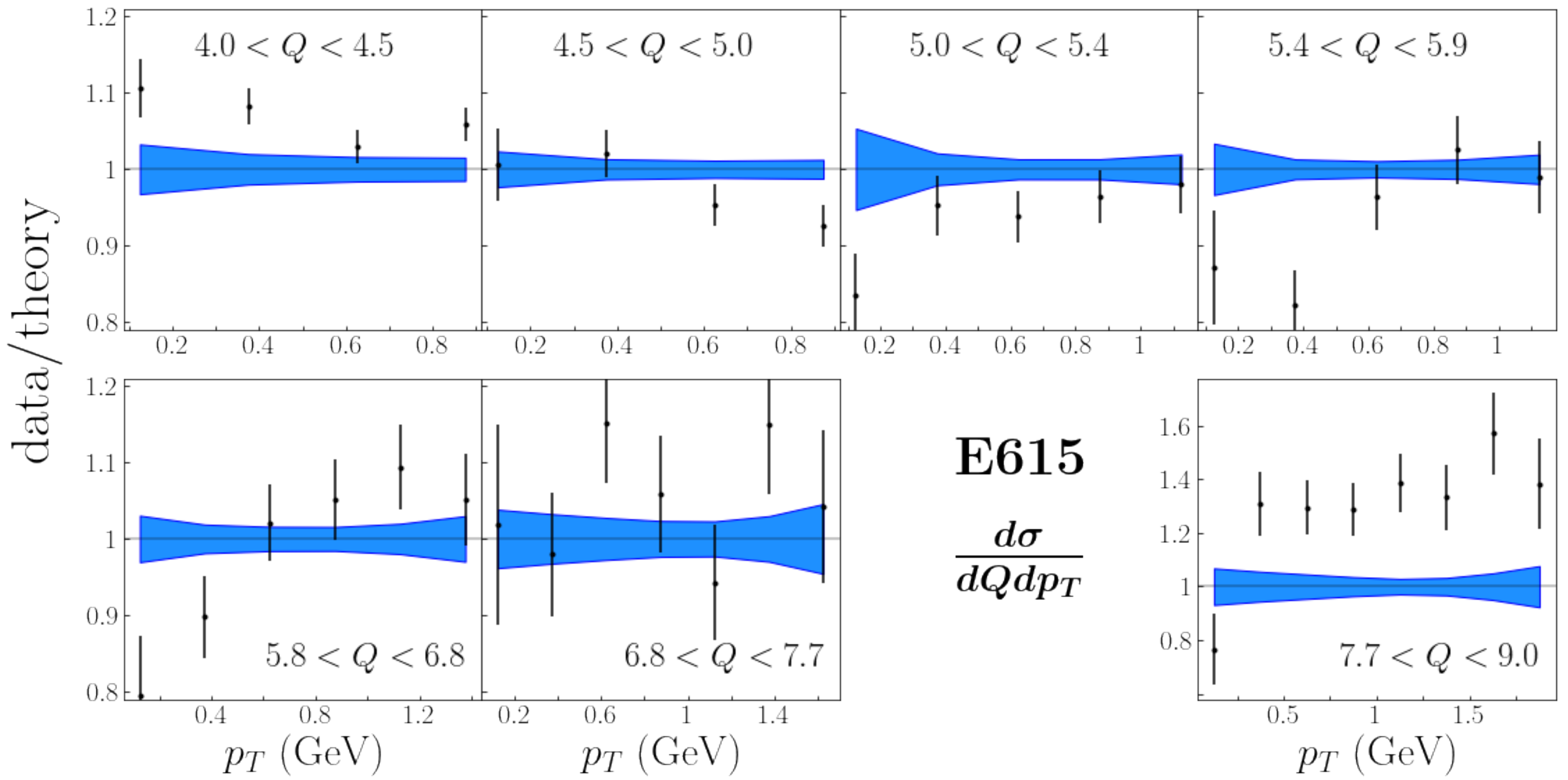

Results …

Process	Experiment	Observable	$N_{\rm dat}$	$\overline{\chi}^2$
$\boldsymbol{pA}$ DY	E288 (200 GeV)	$Ed^3\sigma/dp^3$	38	1.04
Platinum	E288 (300 GeV)	$Ed^3\sigma/dp^3$	38	1.49
	E288 (400 GeV)	$Ed^3\sigma/dp^3$	34	1.38
Copper	E605	$Ed^3\sigma/dp^3$	19	1.56
$\boldsymbol{\pi A}$ DY	E615	$d^2\sigma/dQdp_{\rm T}$	39	4.21
	E615	$d^2\sigma/dx_Fdp_{\rm T}$	48	1.46
	E537	$d^2\sigma/dQdp_{\rm T}^2$	37	0.80
	E537	$d^2\sigma/dx_Fdp_{\rm T}^2$	45	1.00
$\boldsymbol{\pi A}$ DY	E615	$d^2\sigma/dx_Fd\sqrt{\tau}$	61	0.81
	NA10 (194 GeV)	$d^2\sigma/dx_Fd\sqrt{\tau}$	36	0.55
	NA10 (286 GeV)	$d^2\sigma/dx_Fd\sqrt{\tau}$	20	0.95
LN	H1	$F_2^{\rm LN(3)}$	58	0.48
	ZEUS	R	50	1.39
Total		–	**523**	**1.28**

A first fit simultaneous fit of pion TMD & pion collinear pdf

Preliminary

What was done here was to fit to all pion and pA DY data *and* fit the gK and proton gJ’s along with pion gJ’s and pion PDFs. Chi^2 and data/theory plots are from this step - including both pion and proton data.

Collinear
- DY E615 p_{T} integrated
- NA10
- LN/Sullivan H1 & ZEUS (HERA)

Low p_{T}
- DY E615 p_{T}
- DY E537
- pA DY - E288, E605

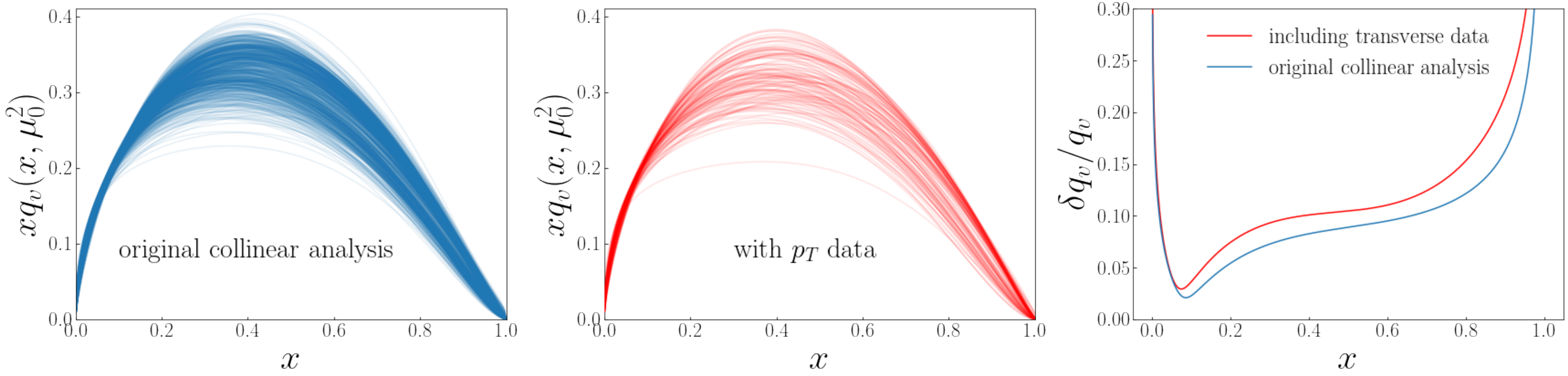

Resulting TMDPDFs

- d quark in the π^- is in the valence region — majority of the DY region
- Shown at a representative $Q = 6$ GeV and $x = (0.1,0.3,0.6)$

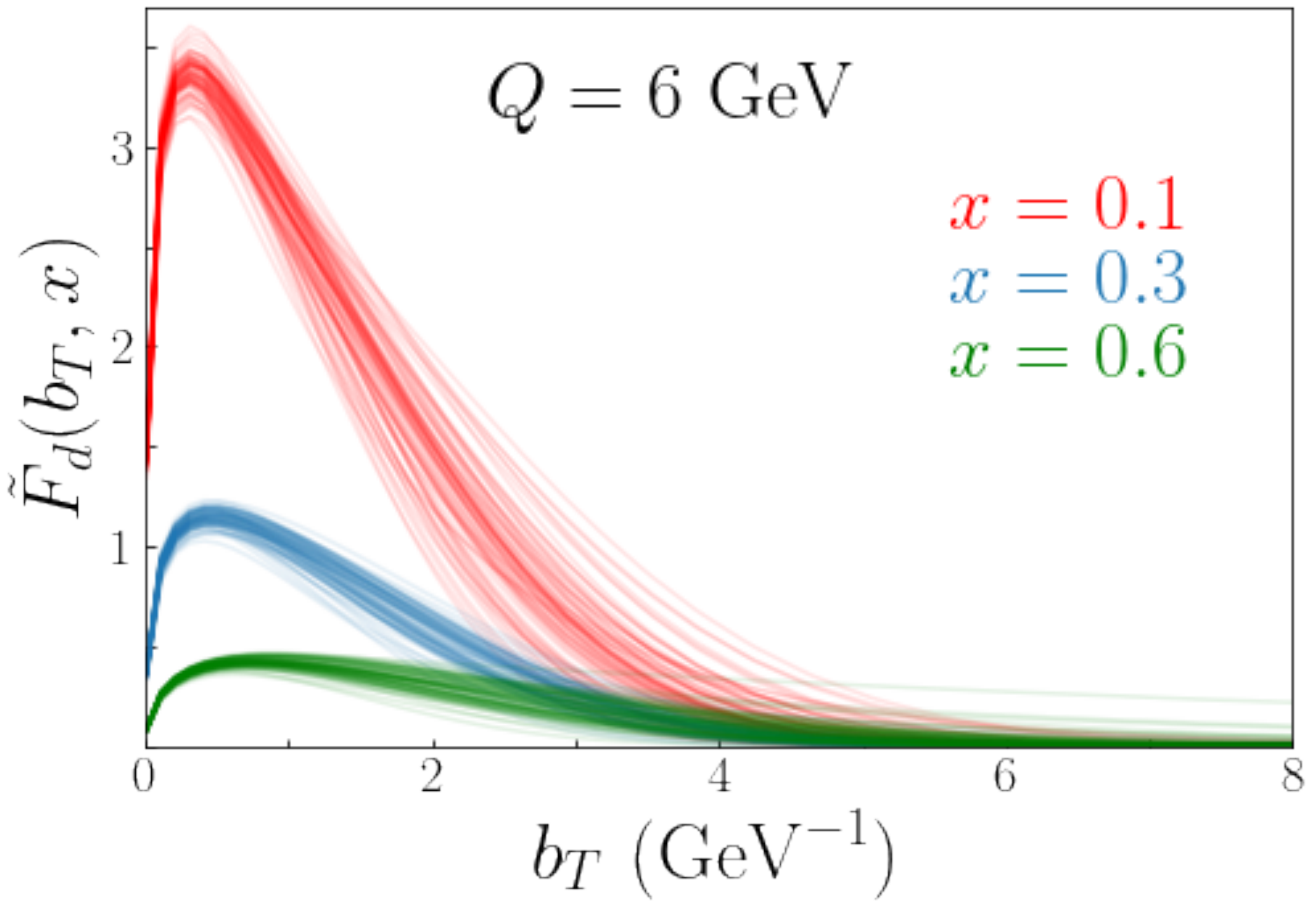

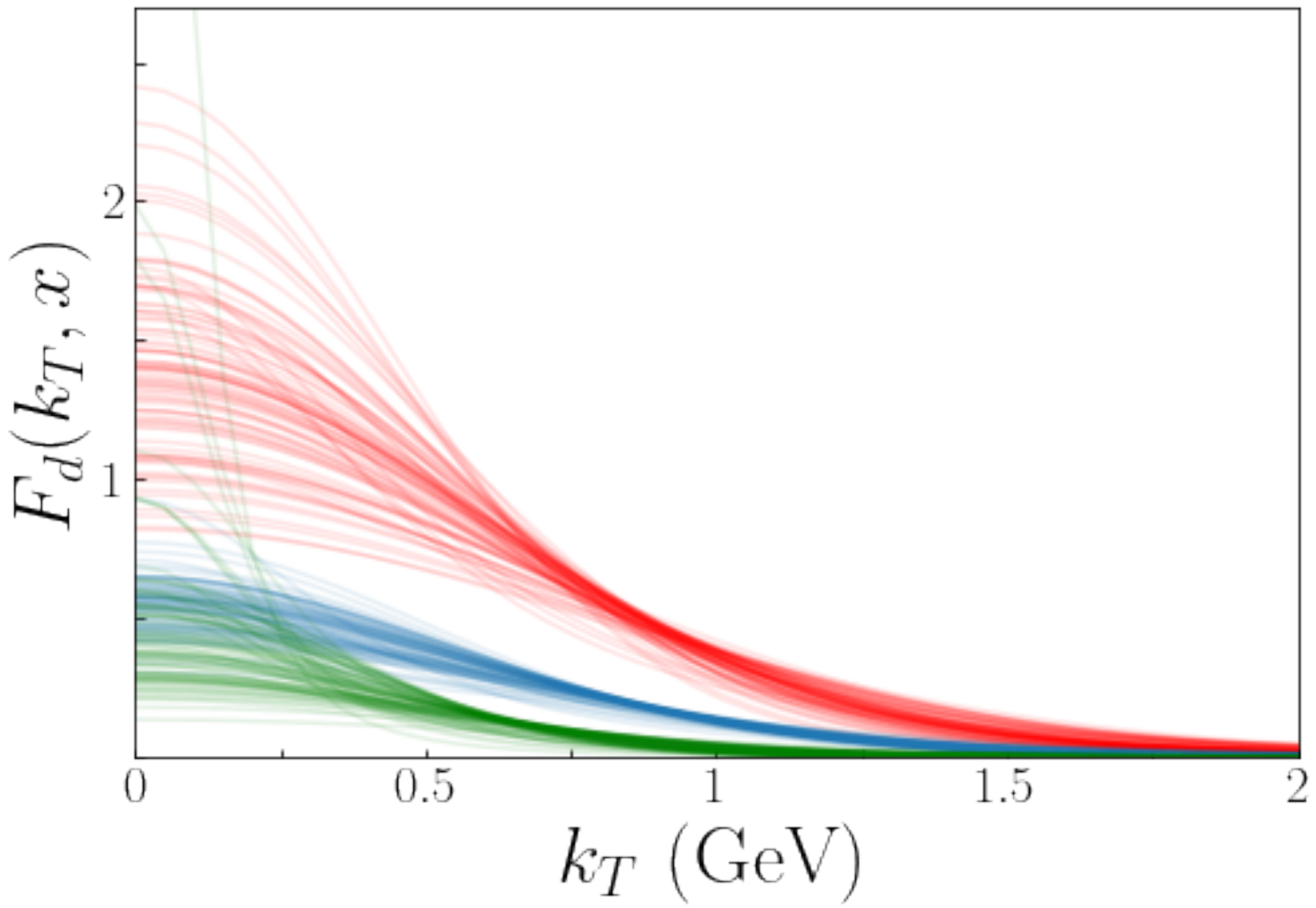

Calculation of the Collins Soper Kernel

$$\tilde{K}(b_T,\mu) = \tilde{K}(b_*,\mu) - g_K(b_T,b_{max})$$

N2LL

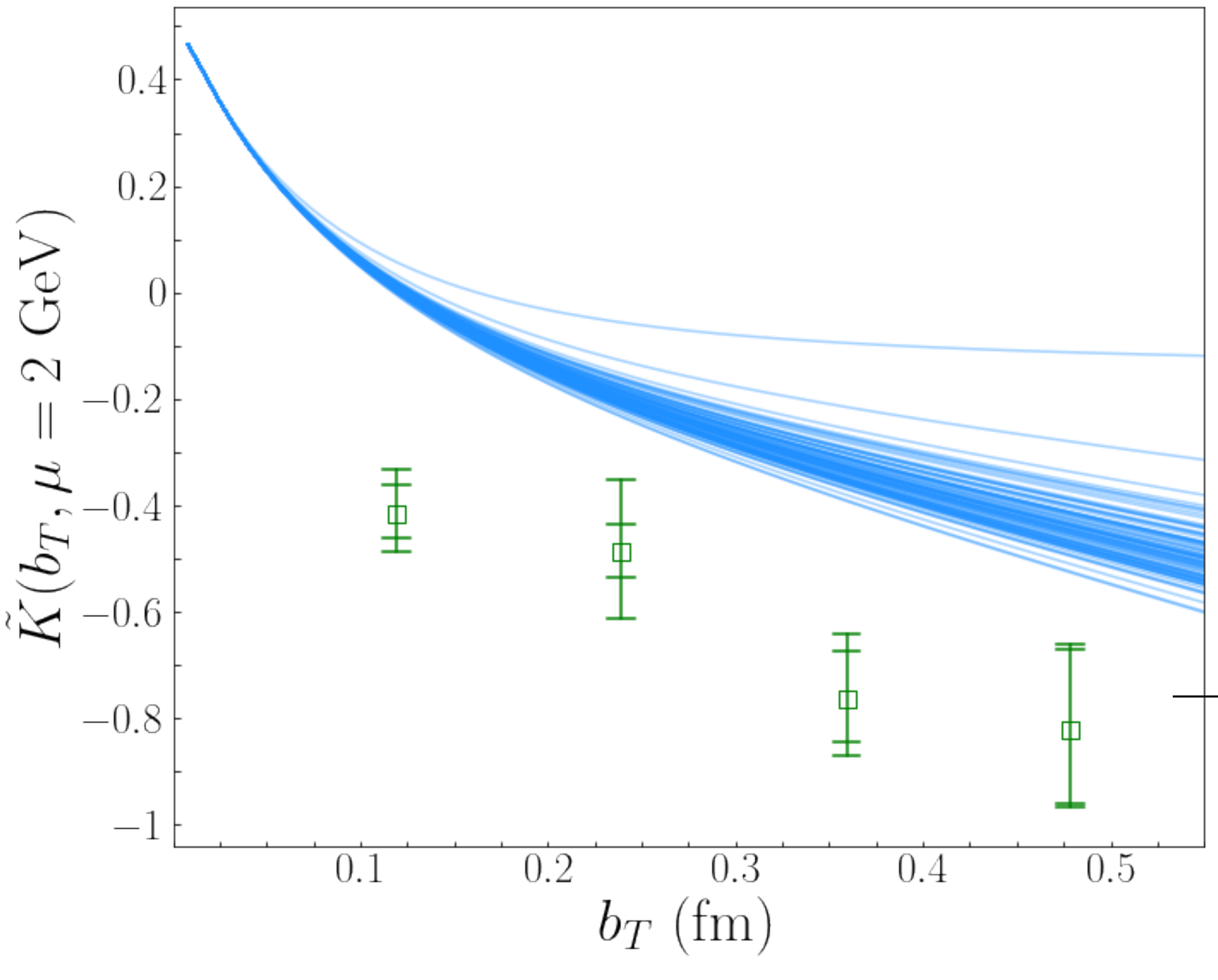

Shanahan, Wagman, Zhao, *PRD* (2020)

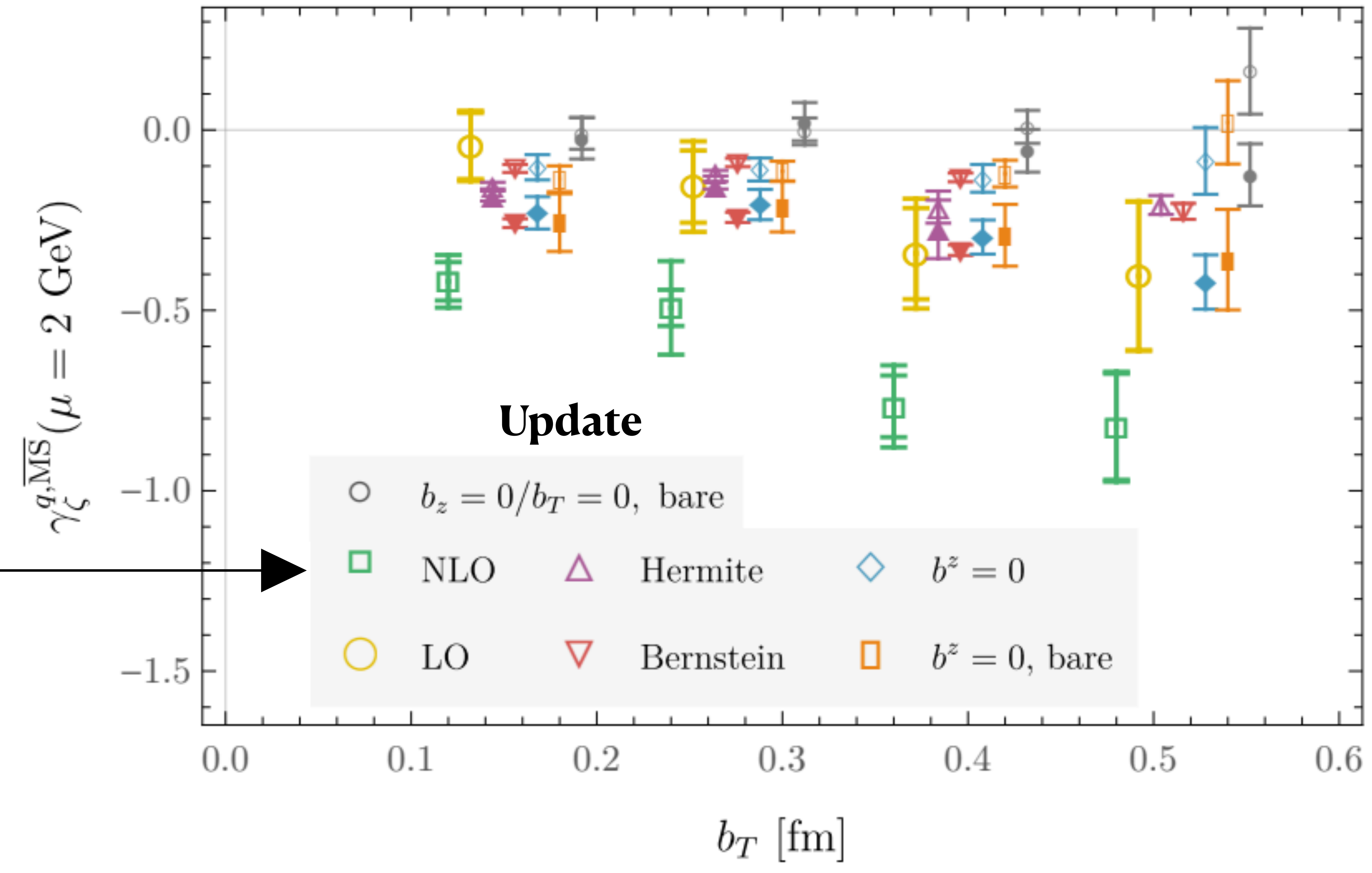

Correlation matrix

Notice the lack of correlation between PDF parameters (above red line) & TMD parameters (below red line)

Lack of correlation indicates the low-p_T data only constrain the TMDs

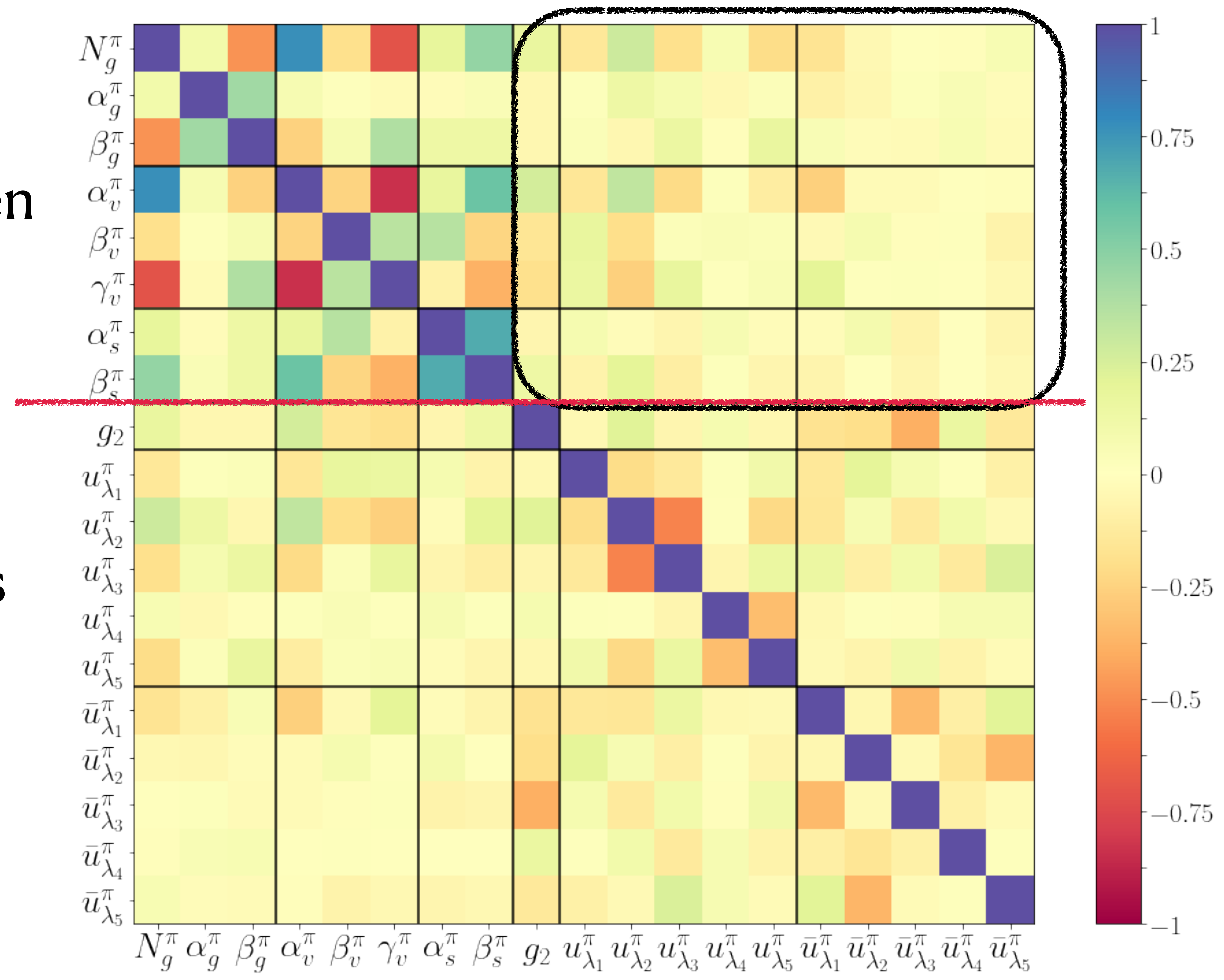

Further Comments

- Our prelim M.C. fit performed w/ flavor separation N²LL $p_{T\,max} = 0.25\,Q$
- Total χ^2/npts=1.28
- Low p_T π-induced DY data constrain the π TMDs but *not* the collinear PDFs
- Correlation matrix showed lack of (anti)correlation between PDF and TMD parameters, indicating lack of sensitivity of the PDFs in determining TMDs
- Further analyses can be performed to test sensitivity to TMD modeling

Summary

- Performed a new Monte Carlo analysis of pion parton distribution functions including for the first time fixed target p_T dependent π-nuc DY cross section data at moderate to low scales together with p_T integrated DY data and LN data.
- This study provides a first simultaneous analysis of collinear and transverse momentum dependent pion distributions
- Provides a first glimpse of the interplay of non-perturbative transverse momentum properties through pion transverse momentum dependent parton distribution functions on collinear pion pdfs.
- Also, studying in various NP schemes NP schemes, flavor dependence, ...

★ Future entails the study of matching low and hi p_T data

1) $$\frac{d\sigma^{DY}}{dQ^2 dy} = \sum \int dx_a\, dx_b\, H^{DY}_{a,b}(x_a, x_b, y, Q^2, \mu^2)\, f_{a/A}(x_a, \mu^2)\, f_{b/B}(x_b, \mu^2)$$

2) $$\frac{d^3\sigma^{LN}}{dx_B\, dQ^2\, dx_L} = \frac{4\pi\alpha^2}{x_B\, Q^4}\left(1 - y_e + \frac{y_e^2}{2}\right) F_2^{LN}(x_B, Q^2, x_L)$$

3) $$\frac{d\sigma^{DY}}{dQ^2 dy dp_T} = \sum_{a,b} \int dx_a\, dx_b\, H^{FO}_{a,b}(x_a, x_b, y, p_T, Q^2, \mu^2)\, f_{a/A}(x_a, \mu^2)\, f_{b/B}(x_b, \mu^2)$$

4) $$\frac{d\sigma^{DY}}{dQ^2\, dx_F\, dp_T^2} = \frac{d\sigma^W}{dQ^2\, dx_F\, dp_T^2} + \mathcal{O}(p_T/Q)^a$$

4"+") $$\frac{d\sigma}{dQ^2\, dx_F\, dp_T^2} = \frac{d\sigma^W}{dQ^2\, dx_F\, dp_T^2} + \frac{d\sigma^{DY}}{dQ^2\, dx_F\, dp_T^2} - ASY\,(\text{double count})$$

$$= \quad W \quad + \quad Y$$

Extras

Suspicious behavior of sea quark TMD

- The $g_j(b_T)$ should allow an integrability of b_T from $0 \to \infty$, and when negative at large b_T, cannot be integrated over all b_T to infer TMDPDF
- Certain regions of x indicate this may not be possible from the sea quark level
- Not obvious in fits because of contraction with tungsten TMDPDF
- We are investigating further with a penalty to dissuade fitter from allowing these solutions

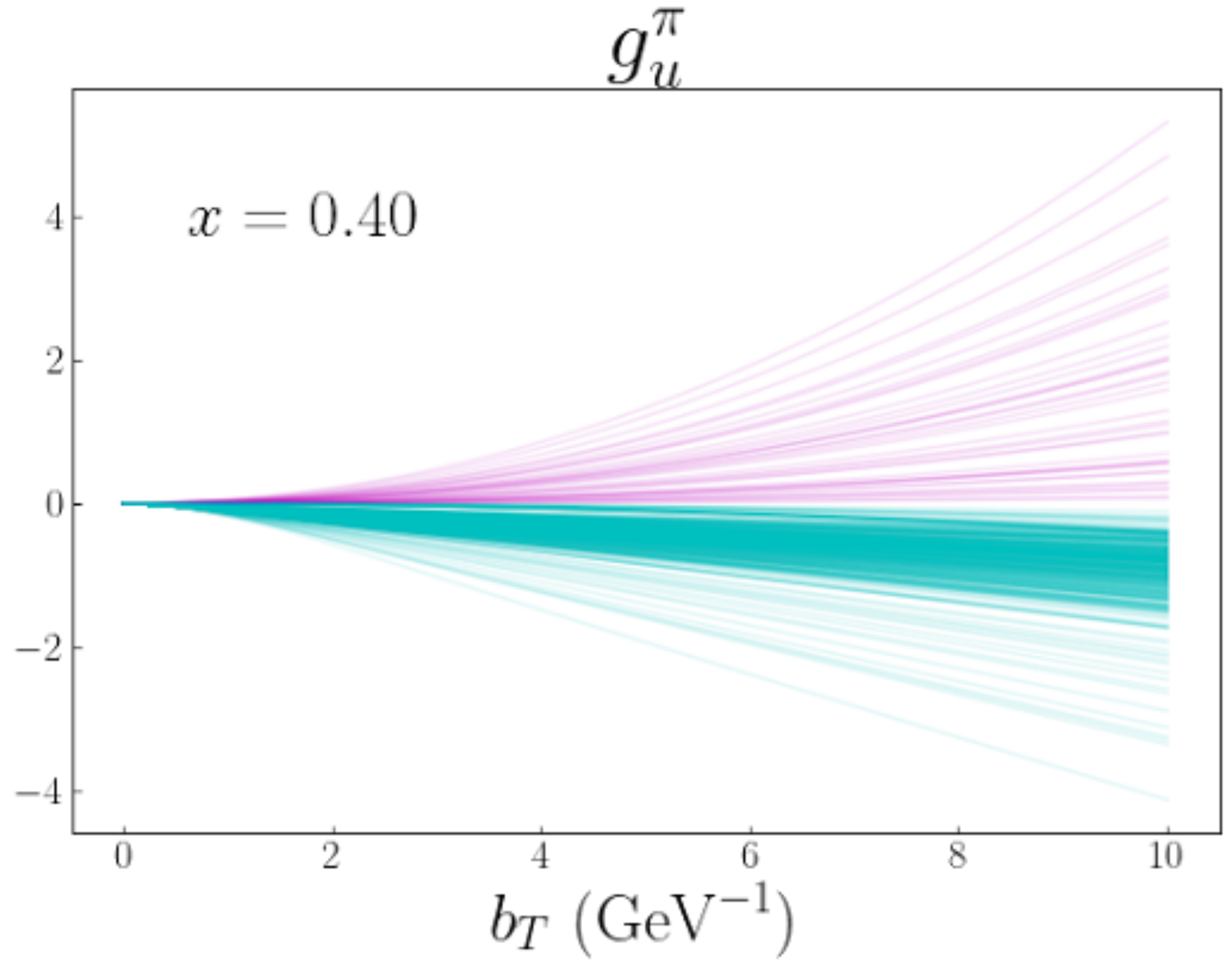

Nuclear Dependence

Table 1

F_{u/p/A} = R_u * F_{u/p}
F_{d/p/A} = R_d * F_{d/p}
F_{u/A} = Z/ A * F_ {u/p/A} + (A-Z)/A * F_{d/p/A}
F_{d/A} = Z/ A * F_ {d/p/A} + (A-Z)/A * F_{u/p/A}

Rs from *Eur.Phys.J.C* 77 (2017) 3, 163
Kari J. Eskola, Petja Paakkinen, Hannu Paukkunen, Carlos A. Salgado

Beyond the W term MATCHING p_T in CSS

✦ *Collins Soper Sterman NPB 1985*

✦ *Collins 2011 Cambridge Press*

✦ **Collins, Gamberg, Prokudin, Sato, Rogers, Wang PRD 2016 - improved matching**

$$\frac{d\sigma(m \lesssim q_T \lesssim Q, Q)}{dy dq^2 dp_T^2} = \left.\frac{d\sigma^W(q_T, Q)}{dy dq^2 dp_T^2}\right|_{m \lesssim q_T \ll Q} + \left.\frac{d\sigma^{FO}(q_T, Q)}{dy dq^2 dp_T^2}\right|_{m \ll q_T \lesssim Q} - \left.\frac{d\sigma^{ASY}(q_T, Q)}{dy dq^2 dp_T^2}\right|_{m \lesssim q_T \ll Q}$$

$$\equiv W(p_T, Q) + FO(p_T, Q) - AY(p_T, Q) + O\left(\frac{m}{Q}\right)^c$$

$$\equiv W(p_T, Q) + Y(p_T, Q) + O\left(\frac{m}{Q}\right)^c$$

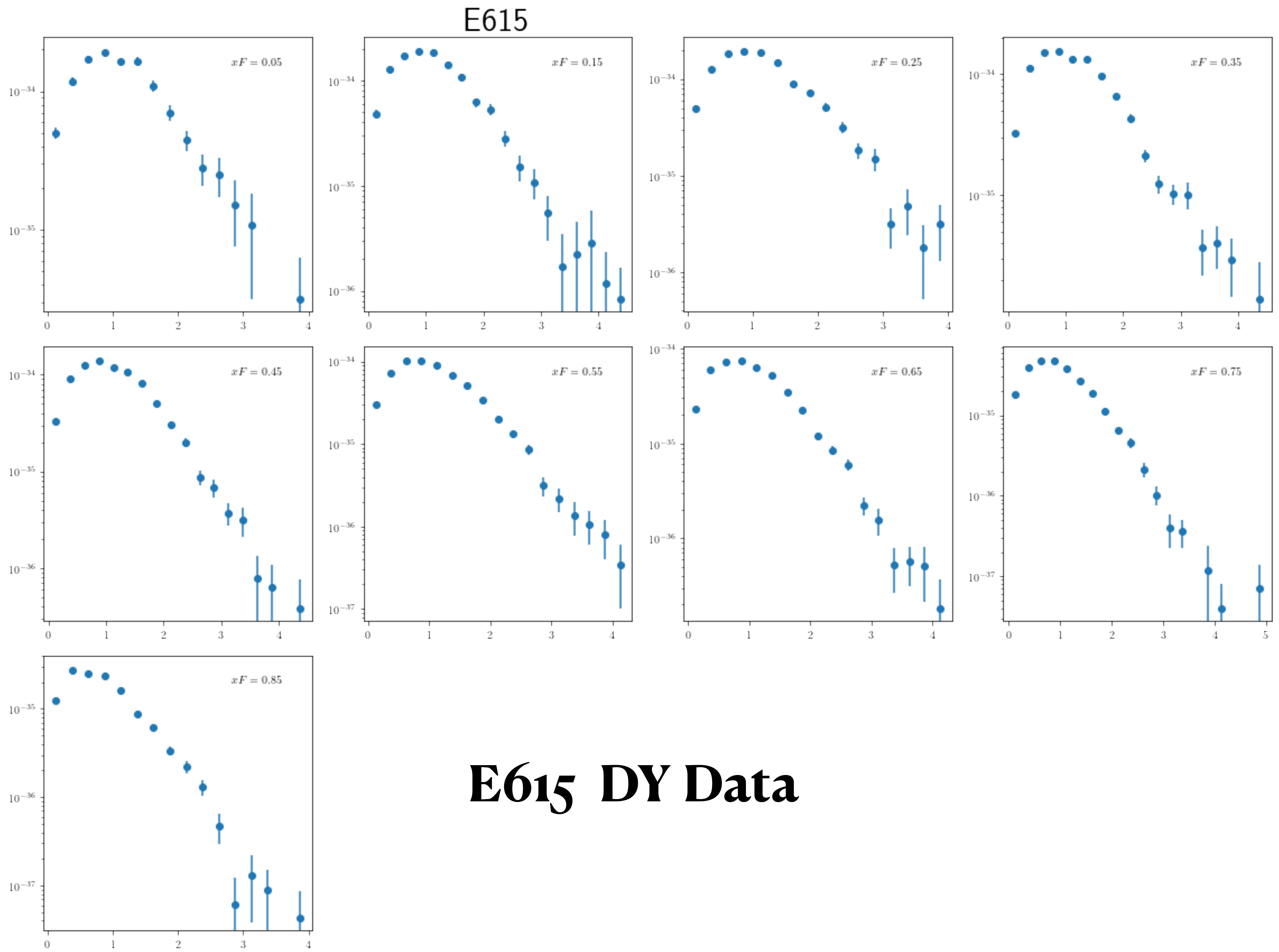

E615 DY Data

- **<u>Cross section in terms of different "regions"</u>**
- W valid for $q_T \sim k_T \ll Q$ TMD factorization
- FO valid for $k_T \ll p_T \sim Q$ Collinear factorization
- ASY subtracts d.c. & in principle
- $ASY \to W,\ p_T \to \infty$ and $ASY \to FO, p_T \to 0$

Drill down ⟶

TMD MC analysis – low energy pA & then π A Drell-Yan data

Using Scheme "1" show some prelim results

$$\frac{d\sigma}{dp_T^2 dy dQ^2} = \sigma_0 \sum_{i,j} H_{i,j} \int_0^\infty db_T b_T J_0(p_T b_T) \times \mathrm{OPE}_{i/A} \times \mathrm{OPE}_{j/B}$$
$$\times e^{S_{\mathrm{pert}}} \times f_{\mathrm{NP,A}}(x_A, b_T) f_{\mathrm{NP,B}}(x_B, b_T) \times \left(\frac{Q^2}{Q_0^2}\right)^{-g_K}$$

$$\tilde{f}^j_{NP}(b_T, x, Q) = \left(\frac{b_*}{b_T}\right)^{2-\nu} \frac{K_{1-\nu}\left(M b_T\, x^{g_1}(1-x)^{g_4}\right) \times (1 + C_A b_T + C_B/b_T)}{K_{1-\nu}\left(M b_*\, x^{g_1}(1-x)^{g_4}\right) \times (1 + C_A b_* + C_B/b_*)}$$

$$\boxed{g_K(b_T) = \frac{g_2}{2} \log(b_T/b_*)}$$